UNIVERSITY OF BIRMINGHAM

SCHOOL OF CHEMISTRY

MRes

Project Report

Preparing Biological Surfaces with Well-defined Density and Spatial Distribution

Akash Beri

May 2010

Abstract

The objective of this project is to fabricate a surface that is optimally spaced and well-defined, with respect to the molecular components to enable efficient binding from the surface. This binding will be done using supramolecular interactions and the steric bulk of dendrons (to achieve the spacing). In order to do this, the axle component of a pseudorotaxane complex would have to be synthesised and absorbed to the surface *via* covalent bonding (chemisorption) to create a self-assembled monolayer (SAM). This is spaced out by the steric bulk of the dendrons which is attached to the wheel component of the pseudorotaxane complex, that is hydrogen bonded to the axle. The pseudorotaxane complex will then disassemble by pH modulation leaving behind spatially separated chemisorbed axle components and simultaneously the vacant surface space will be filled with tri ethyelene glycol thiol terminated alkane thiol (TEGT) creating an optimally spaced SAM.

The first part of this research involved the synthesis of a crown ether (the wheel component) covalently attached to a bulky dendron (**Scheme 3.3**, compound **12**). Successful synthesis was achieved over a five step procedure, allowing the complexation part of the research to take place.

The next part of the research involved the complexation of dibenzo [24] crown 8 (DB24C8) with a dialkylammonium thiol, **1**, and the complexation of **12** with a dialkylammonium thiol, **1**, to form pseudorotaxane like complexes. Both complexation reactions were completed, indicated by the ^{1}H NMR showing both the pseudorotaxane complex and the starting materials. Therefore, further work is required in the complexation step, as any uncomplexed dialkylammonium thiol, **1**, will have an effect on the spacing of the SAM.

SAM formation of the single components (**1** and triethylene glycol, **2**) involved in the mixed monolayer were monitored and characterised over a 24 hour time period by a combination of contact angle, ellipsometry and X-ray photoelectron spectroscopy (XPS). Results indicate that for both components higher molecular ordering was achieved when the immersion time was 24 hours.

During the research two control studies were conducted on gold (Au) surfaces and were characterised by contact angle and ellipsometry. Results indicate that **12** had no major affinity to Au surfaces and that TEGT, **2**, can displace a fully formed dialkylammonium thiol, **1**, SAM. Further work is required to confirm that there is zero affinity between **12** and Au surface and to find out to what extent the TEGT displaces the dialkylammonium thiol.

Contents

Page

Acknowledgements

There are many people who I would like to thank for their help and support during both the research and writing up of this thesis.

Firstly I would like to say thank you to both my supervisors, Professor Jon A. Preece and Dr Paula M. Mendes for their help, advice, supervision and motivation throughout my research masters. Thanks must also go to the members of both the Preece and Mendes group past and present, namely Dr Parvez Iqbal, Scott Charlesworth, Dr Mayaandithevar Manickam, Dr Christopher Hamlett, Simon Leigh, Cheng Yeung, Alice Pranzetti, Vivek Davda, Cait Castello, Minhaj Lashkor and Rachel Allen.

Away from my group I would like to thank Mr P. Ashton, Mr N. May, Ms L. Hill and Dr N. Spencer for their analytical help throughout my research. I would also like to thank Dr J. Bowen for his training and help on all the surface analysis equipment (contact angle and ellipsometry) used in the thesis.

Finally, I would like to say thank you to my family, Ashok, Sumita, Sanjeev and Chaya Beri for all their help, support and encouragement throughout my studies.

1.0 Introduction

1.1 What is Nanoscience?

"Nanoscience or nanoscale science has been defined as the chemistry and physics of structures with dimensions in the length scale of 1-100 nm[1]." Nanoscience is a multidisplinary science which pulls together chemists, physicists, engineers and biologists. This area of research has had an impact on nearly all scientific and engineering sub disciplines by creating structures with well defined properties through control of nanoscale architectures[2].

The birth of nanoscience can be attributed to Nobel Prize winner Richard Feynman who gave a talk in the late fifties which suggested that the manipulation of matter down to the atomic scale is possible[3]. Since the fifties there has been great advance in nanoscience and in 1974 the field was termed 'nanotechnology' by Norio Taniguchi[4].

1.2 Nanotechnological applications

The use of nanoscale devices has huge scope for nanotechnology. Two main areas where this technology has been utilised are the electronics industry and the pharmaceutical industry.

1.2.1 Electronics industry

Over 40 years ago the first integrated circuit was created and since then the number of transistors on a silicon chip has doubled every 18 months[5]. This is a direct result of the size of the transistors decreasing. The minituarisation of these devices in the microelectronics industry has led to smaller and more powerful devices being created.

1.2.2 Pharmaceutical industry

Nanotechnology has also been applied in the pharmaceutical industry. It can play a crucial role in analysing biological structures which could lead to better treatments for patients. In

addition in 2009 Nielsen *et al.*[6] were investigating the use of cyclodextrin nanoparticles as carrier molecules to control the drug release within the body. This would significantly reduce the side effects of drugs. More research is still required but it is a promising methodology for reducing the amount of side effects a drug can cause.

1.3 Two dimensional ultrathin films

Ultrathin thin films are two dimensional well-ordered molecular assemblies used to fabricate nanoscale platforms[7]. The films provide a simple, cheap and reproducible method of obtaining nanoscale thick films which can be chemically manipulated[8], thus making ultrathin films suitable for applications in the electronic and pharmaceutical industry.

Two types of ultrathin films used for such potential applications are Langmuir-Blodgett films[8] (LBFs) and self-assembled monolayers[9] (SAMs), for the purpose of this thesis only SAMs will be discussed.

1.4 Self-assembled monolayers

Self-assembled-monolayers (SAMs) (**figure 1.1a**) have been used for many years in a variety of applications including biosensors[10], thin film resists[11] and assays[12]. SAMs are ordered structures that form spontaneously when a surfactant (**figure 1.1b**) is adsorbed onto a substrate[12].

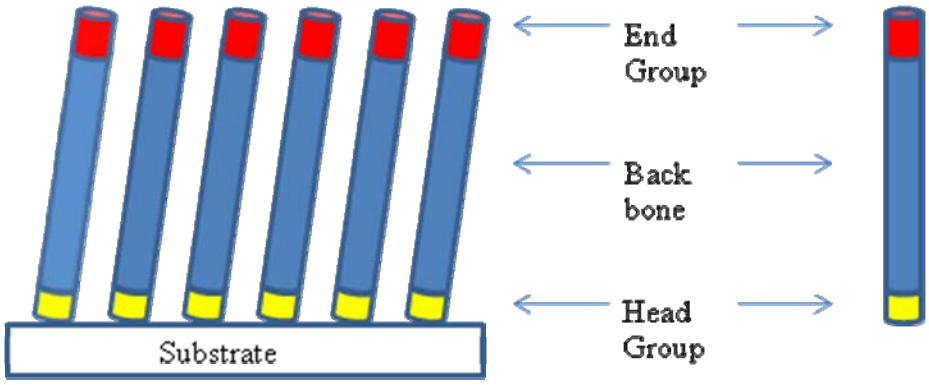

Figure 1.1 – Schematic of (a) SAM and (b) the surfactant.

1.4.1 Substrate

The chosen substrate needs to be able to provide sites on the surface where chemisorption (i.e. covalent or ionic bonding) occurs with the head group[7]. There are two main surfaces used when making SAMs, gold (Au) and silicon oxide (SiO_2)[7]. If Au is used then the head group will be a thiol and if SiO_2 is used then a silane will be used as the head group. The choice of the surface depends on the practicality of use and strength of adsorption required for the desired application.

Sulfur – Au

Sulfur binds extremely well to Au, Au (111) is favoured over Au (001) as it has a lower surface energy[7]. Thiol SAMs are the most commonly used as they are easy to prepare and analyse[12, 13], they form highly organised SAMs[7] and they can be prepared under ambient conditions[7].

Silane – SiO_2

It has been found that silane SAMs are less ordered than thiols on Au[14]. However the silane SAMs are more chemically and thermally stable than thiols on Au surfaces[12]. The increased stability is a direct result of the cross polymerisation between silane head groups[15]. Regardless of the fact that silane SAMs are more stable, thiol based SAMs are more

commonly used, as silane based SAMs with a reactive functional group are harder to form experimentally[12].

1.4.2 Surfactant

The SAM consists of a single layer of densely packed surfactant molecules, the surfactant consists of three elements; the head group, the backbone and the end group (**figure 1.1b**).

Head Group

The head group binds the surfactant to the surface *via* chemisorption[7]. The choice of head group (e.g. thiol, silane) depends directly on what substrate (ie Au, SiO_2) is being used. Each head group will have a different affinity to that particular substrate.

Backbone

The backbone plays a major role in the thermal stability and molecular packing of a SAM[16]. The backbone is generally made out of an aliphatic chain and/or an aromatic component.

Each molecule in the SAM interacts with neighbouring molecules through the backbone. The molecules can interact by van-der-Waals and π-π interactions which lead to a relative well-ordered molecular layer being formed.

As SAMs are two-dimensional quasi-ordered molecular assemblies[7], the backbone components exist in both the x and y axis resulting in a tilt angle. This angle can vary depending on the chain length[7].

End Group

The end group plays a role in providing a SAM with its surface properties for different applications, such as wetability[17], corrosion susceptibility[18] and biomolecular immobilisation[19].

1.5 SAM Formation

When a surface is immersed in a solution containing a surfactant, self-assembly occurs, which results in the formation of relatively ordered, closely packed and stable monolayers[7]. There are several experimental parameters that can dictate the formation of SAMs. These parameters include; surfactant concentration[20], substrate[7], temperature[21], time[21], solvent[20, 21], atmosphere[21] and surface morphology[7]. The process of self-assembly occurs in four steps (**figure 1.2**) resulting in the absorption of surfactant onto the surface of the substrate[7].

1. In the first step of SAM formation, physisorption begins between the surfactants in solution and the surface. This results in the surfactant molecules lying parallel to the surface of the substrate.
2. In the second step, chemisorption begins between the head groups of the surfactant and the surface forming a relatively strong chemical bond (either covalent or ionic). Chemisorption is an exothermic process that results in the pinning of a surfactant head group to a specific site on the surface through a chemical bond. This pinning can be a Si-O bond in the case of organosilanes on hydroxylated SiO_2 surfaces[22], or a Au-S bond in the case of alkanethiols on gold[23]. The rate of chemisorption is time dependent, and will vary depending on what surfactant and substrate is being used. It has been found[7] that 80-90% of full surface coverage occurs in the first few minutes of immersion.

3. In the third step molecular ordering begins. This is where the surfactants move closer together on the surface, allowing intermolecular interactions to occur between the backbones of the surfactant. These interactions allow the SAM to become closely packed and ordered.

4. In the final step further ordering can occur, this can take place after a few days or months[7].

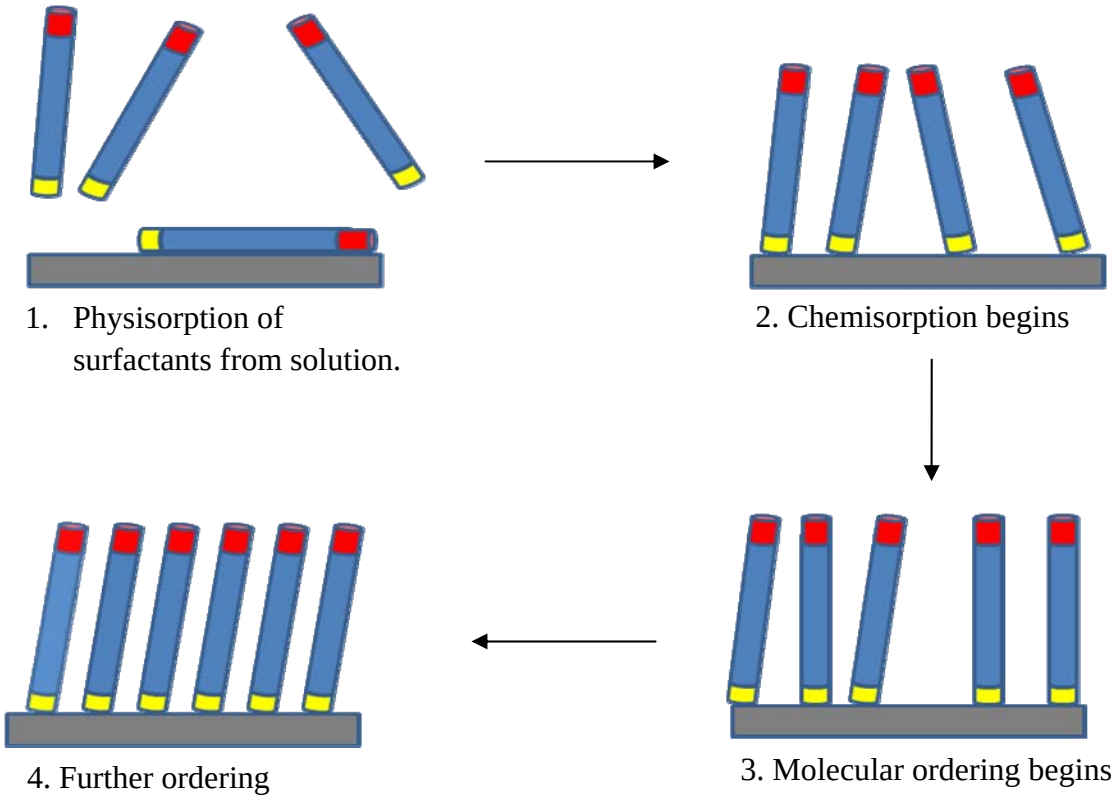

Figure 1.2 – Schematic of SAM formation.

Throughout this four step process there are many different energies[24] involved with the overall SAM formation, these are indicated in **figure 1.3**[24]. During SAM formation the biggest energy change occurs when the surfactant absorbs onto the surface. This energy is a direct result of the head group of the surfactant chemisorbing to the surface of the substrate. This absorption energy (ΔE_{ads}) is the strongest energy involved and it is this energy which contributes the most to self-assembly. The substrate corrugation energy (ΔE_{corr}) refers to the energy difference between the different absorption sites. After the surfactants chemisorb to

the surface they have some surface mobility. The lower the ΔE_{corr}, the closer the packing of the surfactants. Once the surfactants get in close proximity, intermolecular forces (e.g. Van der Waals) between the backbones (ΔE_{hyd}) of the alkyl chains can occur causing an increase in surface coverage. This chain-chain interaction is crucial in the packing of the monolayer. The final energy that is involved is the defect energy (ΔE_g) otherwise known as the gauche defect which is caused by the backbone not fully extending.

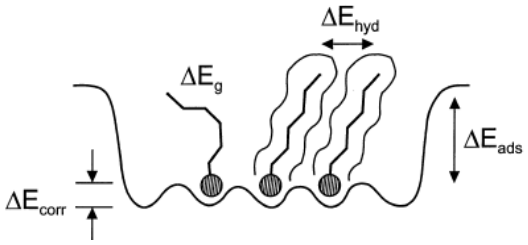

Figure 1.3 – Schematic of energies involved in SAM formation[24].

1.6 Two Component SAMs

The formation of two component SAMs is more complicated than the formation of single component systems. There are two main methodologies for preparing two component SAMs[25]. One method involves using various techniques, such as UV irradiation[26-29], UV photolithography[30-32], electron beam bombardment[33] and micro-contact printing[34]. The other technique involves the spontaneous formation of structured monolayers through the co adsorption of surfactants from a mixed component solution[25, 35, 36] or by replacement of absorbed thiols[37]. Co adsorption using a mixed component solution is the preferred technique and is the method generally used[38].

Over recent years, two component SAMs have been used to provide surfaces that not only resist the adsorption of specific biological molecules, but can also have end groups that bind

specifically to biomolecules[39]. This functionality allows two component SAMs to have a wide number of biological applications, such as biosensors[10].

Figure 1.4[13] illustrates how a mixed SAM can be used to interact with a receptor. It shows that by altering the end group of surfactant A, it can bind to a receptor, which can then bind to the appropriate ligand. The size of receptors can vary, therefore the space between two surfactants A molecules needs to vary to allow enough space for the chosen receptor to bind. The choice of the surfactant B is crucial for two reasons 1) it needs to control the space between two surfactant A molecules and 2) it needs to remain inactive once SAM formation is complete.

Oligo-ethylene glycol (OEG) thiols have been found to be ideal for this purpose, as they provide surfaces that do not adsorb proteins[40, 41]. OEG thiols also have other unique properties such as hydrophilicity[42], high exclusion volume in water[42], nontoxicity[42] and nonimmunogenecity[43] which can be utilised when attempting to mimic biological conditions.

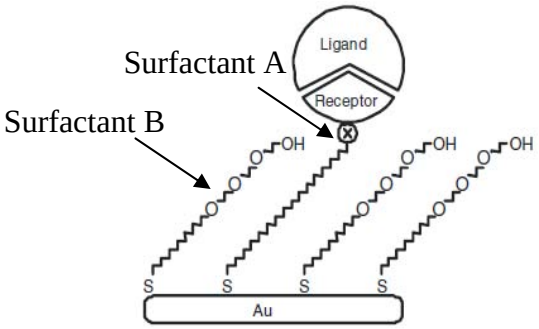

Figure 1.4 – Example of SAM based bio-interfaces[13].

1.7 Current Research

In 2006 Gujraty *et al.*[44] fabricated two component SAMs containing 1-mercaptoundec-11yl hexa(ethylene glycol) thiol and a chloroacetylated derivative of 1-mercaptoundec-11yl hexa(ethylene glycol) thiol from a mixed surfactant solution. This fabricated mixed SAM was

then modified using a cysteine-derivatised peptide containing the integrin-binding tripeptide sequence Arginine-Glycine-Aspartate (RGD). The RGD sequence is commonly found in extracellular matrix proteins and mediates binding to integrins present on the cell surface. RGD-integrin is vital for cell attachment, growth and differentiation[44]. Therefore the modified SAMs were used to mediate biospecific cell adhesion. This was done by incubating the modified monolayer with NIH 3T3 fibroblast cells for a period of 4 hours. After which cell adhesion was monitored using a Nikon microscope. Results indicate that cell adhesion was observed on the RGD-functionalised SAMs. Thus proving that mixed SAMs can be used to mediate biospecific cell adhesion.

In 2008 Choi and Murphy[45] used mixed SAMs to show noncovalent DNA immobilisation and cell adhesion. To do this, multi component SAMs were fabricated using a mixed solution of tri ethylene glycol thiol terminated alkanes (TEGT) and cDNA containing alkanethiols. They were then incubated with target DNA to allow for noncovalent immobilisation. DNA-DNA binding was then analysed using a Biacore spectrometer, which showed that noncovalent DNA immobilisation had been successful. The mixed monolayer was then modified to contain a GGRGDSP peptide and incubated with C166-GFP endothelial cells to test for cell adhesion. Results indicated that cell adhesion occurs for all mixed monolayers containing the GGRGDSP peptide. The research showed that mixed monolayers containing immobilised peptide and TEGT which provide a bioinert background, have potential use as biosensors and DNA delivery platforms[45].

As shown in the two examples, current methodology fabricates multi component SAMs by simply immersing a substrate into a solution containing at least two different surfactants. With this technique, a SAM is created whereby the surfactant with the desired functionality is randomly distributed across the surface. This will either lead to a random distribution of

protein across the surface or it will create a surface where there is not enough space for a protein to interact. As a result of this methodology there are limitations that may occur, these are discussed below.

1.8 Limitations with mixed SAMS

1.8.1 Phase separation

It has been found that phase separation occurs spontaneously within a mixed solution of surfactants[46]. Studies have demonstrated that surfactants with weak interacting molecules which self assemble on the surface, can phase separate into discrete molecular domains on the nanometer scale[47]. As a result of the formation of these molecular domains, the desired distribution of surfactants cannot be achieved and therefore the mixed monolayer will not be ideally ordered or have the desired density.

1.8.2 Ratio Irregularities

As previously discussed, the current methodology for creating a mixed monolayer involves using a mixed surfactant solution. In this methodology the surfactant ratio is chosen so that when the surfactants bind to the surface, they bind in a specific distribution to allow maximum receptor-surfactant binding interaction. It has been found however, that the ratio of surfactants on the surface is not reflective to that in the mixed solution[48]. This can have a major affect on the number of receptor-surfactant binding interactions.

The limitations highlighted above can be eliminated using low density SAMs.

1.9 Low density SAMs

Low density SAMs will have a great role in biological applications as they can provide us with well-defined structures which are optimally spaced. This spacing is crucial because

when large molecules (proteins) are introduced to a surface they occupy a surface area dictated by the shape of the molecule and the mode of the binding[49]. Therefore space is required on the surface to allow this binding between the surface active group and the arriving biomolecule.

Recently a few examples of low density monolayers have been attempted using dendrons to provide the spacing across a surface. Dendrons are highly branched three dimensional macro molecules[50] emanating from a focal point[51], with molecular weight of up to several kDa. The dendrons are characterised by having a single reactive function at the focal point. This gives the dendron the ability to undergo orthogonal reactions[51]. The numbers of branching points from the focal point to the terminal groups of the dendron are used to define the generation of the dendron, and the three dimensional size and shape of the dendron[51]. For example, generation 2, G_2 dendrons refer to dendrons with two branching points from the focal point to the terminal groups of the dendrons.

In 2003 Hong *et al.*[52] attempted to use dendrons to create well-defined monolayers with mesospacing of an amino functional group (**Scheme 1.1**), which could be used later for further application. In this study a dendron with nine carboxylic acid end groups and a CBZ group at the apex was bound to an aminosilane surface (**Scheme 1.1, step 1**). The CBZ group was then deprotected using trimethylsily iodide (**Scheme 1.1, step 2**) forming a compact and smooth monolayer with an amino group at the apex. To prove the amino group was available for further interactions it was reacted with 9-anthraldehyde to form an imine, which was apparent in the UV spectra, thus proving that dendrons can be used to create well defined monolayers with mesospacing.

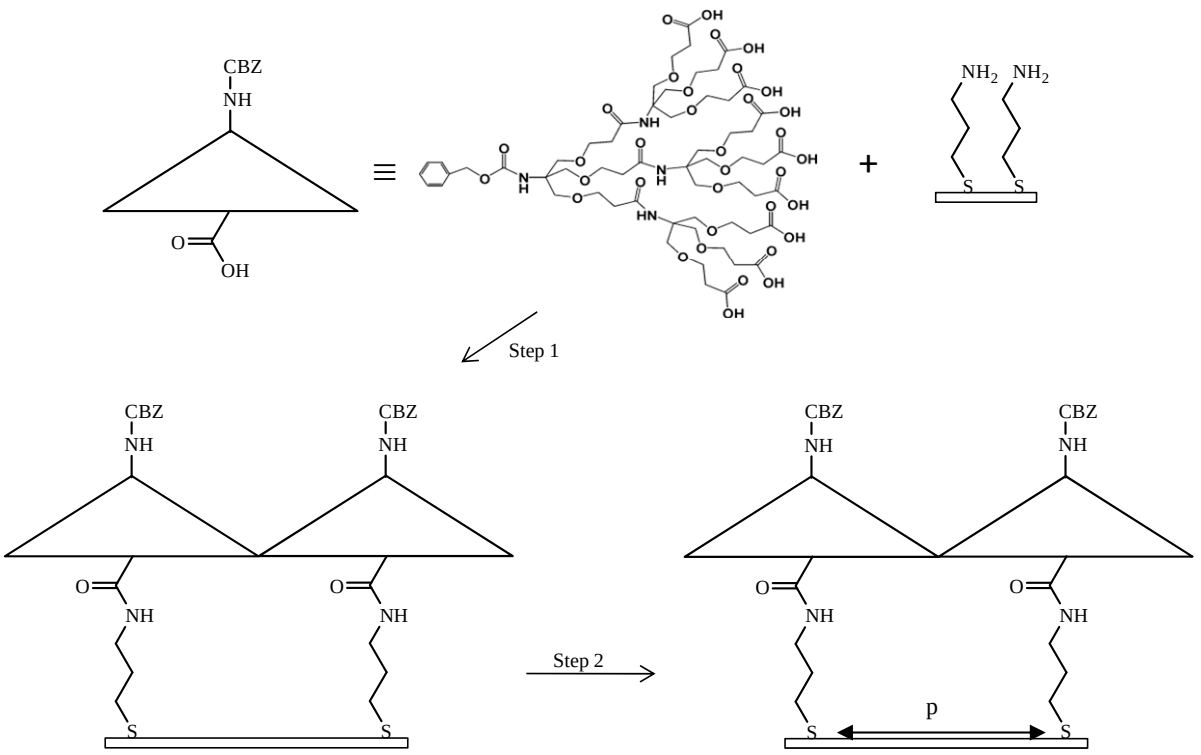

Scheme 1.1 – Schematic presentation of the procedure for the self-assembly of the dendron on an aminosilyated surface (step 1) and the deptrotection of CBZ group by trimethylsilyl iodide (step 2), where p is potential sites for chemisorption which are blocked (figure redrawn from Hong *et al.*[52]).

In 2009 Tokuhisa *et al.*[53] attempted to use dendrons in a mixed monolayer system to fabricate well defined and optimally spaced monolayers. In this study a dendron was attached to an anchor molecule *via* an ester linkage. The other end of the anchor molecule consisted of a thioctic acid group which has the ability to chemisorb to a Au surface. The molecule was then chemisorbed onto a Au surface (**Scheme 1.2a**) and the spacing was controlled by the size of the dendron used. The dendrons were then cleaved *via* hydrolysis (**Scheme 1.2b**), leaving behind spaces between acid terminated chemisorbed components, simultaneously the space was filled with hydroxyl hexane thiol. The carboxylic acid was then activated using N-hydroxysuccinimide (NHS) and 1-ethyl-3-(3-(dimethylamino)-propyl) carbodimide (EDC)

The activated acid was then exposed to NH_2EG-Biotin which produced an optimally spaced and well defined surface which could be utilised in biological applications.

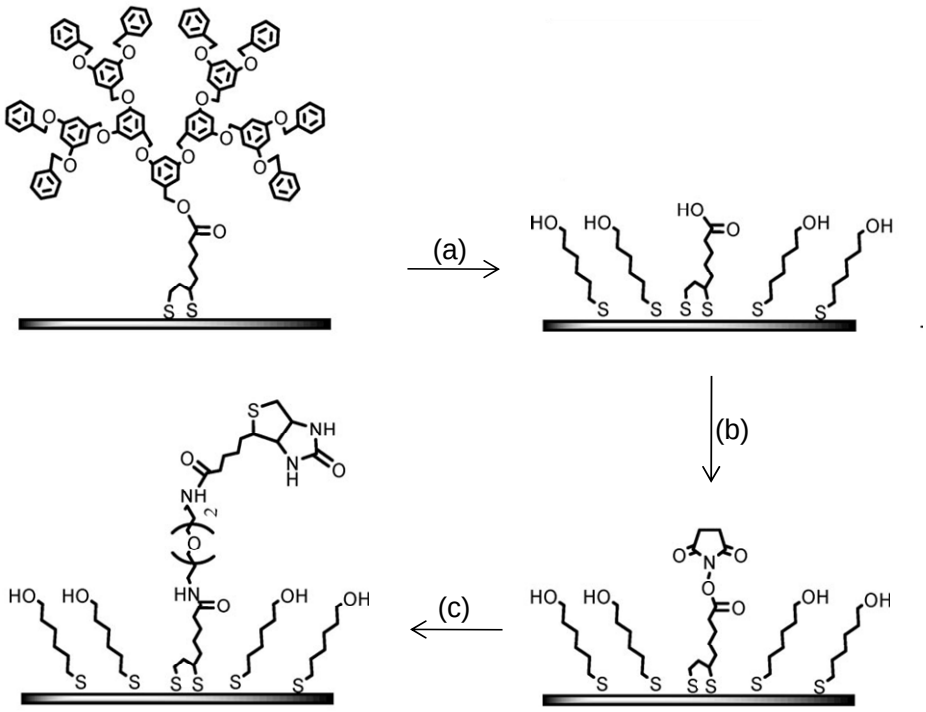

Scheme 1.2 – Schematic drawing for the synthesis of a space-controlled Biotinylated surface from a dendron SAM, where (a) dendron removal *via* KOH hydrolysis, (b) activation of carboxylic acid with NHS and EDC and (c) introduction of biotin moiety through amide formation (figure redrawn from Tokuhisa *et al.*[53]).

To test that the surface could be used in biological applications, the biotin was bound to streptavidin and the amount of binding was monitored using surface plasmon resonance (SPR). For comparison, mixed monolayers were prepared using a mixed surfactant solution of anchor molecule without dendron and hydroxyl hexane thiol. Results indicated an increase of 40% in binding of streptavidin to biotin when using the dendron spacers compared to a 10% binding shown using a mixed surfactant solution.

The study showed that by using dendrons you can enhance the performance of capturing proteins, such as streptavidin, at surfaces by 30%. However in this study, the chemistry used to cleave the dendron, could possibly be damaging the surface and thus depleting the overall binding of streptavidin. Also the study used hydroxyl heaxanethiol to provide the bioinert background, even though previous studies have shown OEGs to be better[40, 41].

The overall aim of my project is to fabricate surfaces that are optimally spaced and well defined utilising the properties of dendrons and supramolecular interactions. The strategy for this is shown in section 3.

1.10 Supramolecular Chemistry

Supramolecular chemistry is defined as "the chemistry of organised entities that result from the association of two or more chemical species which are held together by intermolecular forces"[54]. In molecular chemistry, strong forces (ionic and covalent bonds) are used to bind discrete molecules together[54]. However in supramolecular chemistry weak non covalent interactions (hydrogen bonding, electron donor-acceptor interactions, Van der Waals forces and π–π stacking) are used to assemble molecules. This is known as supramolecular assembly. Self-assembly in supramolecular structures can occur where molecular recognition between a substrate (guest), which has one or more selective binding sites, comes in contact with one or more molecular receptors (host)[54]. A supramolecular structure is formed based on the molecular information of each component[54]. This type of chemistry can be referred to as host-guest chemistry. There are many different macrocyclic molecules that could be used as hosts to create supramolecular structures, such as crown ethers, cyclodextrins, porphyrins and zeolites. The macrocyclic component needs to be a ring structure which has a large enough cavity to allow threading of the guest molecule. It also needs to have the ability to create noncovalent bonding interactions with the guest molecule in order to create a mechanically interlocked supramolecular complex[55]. For the purpose of this research only crown ethers will be discussed.

Crown ethers

Crown ethers were discovered by Pedersen[56] over forty years ago and it was Pedersen who realised their importance in host-guest chemistry[57]. Crown ethers are macrocyclic compounds that consist of a ring containing several ether groups. The size of the ring can be varied depending on the required cavity size needed for threading of the guest molecule. Crown ethers contain oxygen atoms that can undergo hydrogen bonding[58] with the guest molecule to form the desired complex. Over the years various cationic guests[59], such as ammonium ($NH4^+$), primary alkylammonium ions (RNH_3^+) and dialkylammonium ions ($R_2NH_2^+$), have been investigated with crown ethers in order to understand their binding properties[59]. It was found that when dibenzo [24] crown 8 (DB24C8) was used in conjunction with the dialkylammonium ions the dialkylammonium ion can fully interpenetrate the macrocyclic cavity[60] resulting in the formation of a pseudorotaxane complex. Pseudorotaxanes are supramolecular complexes that are mechanically interlocked by noncovalent interactions, therefore they can be threaded and dethreaded by turning the noncovalent interactions 'ON' and 'OFF'.

Threading/dethreading

Figure 1.5 shows a schematic representation of a protonated dialkylammonium ion (guest) threading a crown ether (host) to form a pseudorotaxanes complex. The complex is held together by [N^+-H---O] and [C-H---O] hydrogen bonds and other electrostatic interactions[61]. It has been shown that the substitution of the R groups on the dialkylammonium ion with phenyl rings allows the fine tuning of the supramolecular system[62]. The use of phenyl rings also allows π-π interactions to occur which further stabilises the complex.

Dethreading of the pseudorotaxane complex (**figure 1.5**) is possible on the addition of a base[63], which deprotonates the dialkylammonium ion resulting in the release of the DB24C8.

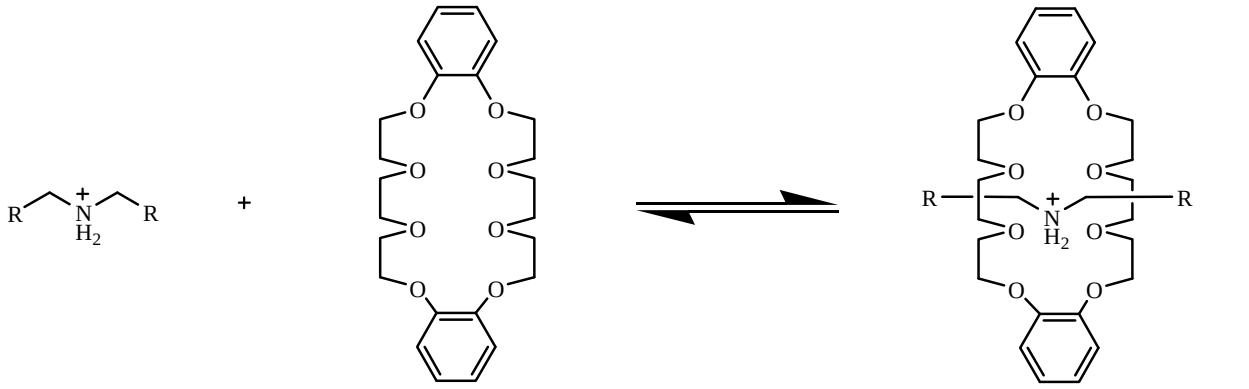

Guest
(axle)

Host
(wheel)

Pseudorotaxane complex

Figure 1.5 – Threading/Dethreading of a host molecule.

The example shown in **figure 1.5** shows a DB24C8 being threaded and dethreaded by altering the pH environment of the dialkylammonium ion. However other stimuli, such as light[64], competitive binding[65] and redox control[66] have been used to thread and dethread host molecules. This versatility allows pseudorotaxane complexes to be utilised in nanovalves[67] which have applications in molecular switches[68] and molecular sensors[65].

2.0 Surface Characterisation

In this section, the surface characterisation techniques that will be conducted on the SAMs are discussed.

2.1 Contact angle

Contact angle measurements supply us with information regarding the wetting behaviour of a surface. This technique is done at ambient temperature and is relatively quick and simple. When a liquid droplet is placed on a solid substrate, equilibrium forces such as interfacial tensions are measured as three phases come into contact, i.e. solid/liquid, solid/vapour, and liquid/vapour interfaces[69]. For example if water is the liquid phase, a hydrophilic surface will exhibit a low contact angle (~20°), whereas in comparison a hydrophobic surface will exhibit a high contact angle (~90°)[7]. There are three ways to measure contact angle, which are sessile drop contact angle measurement, dynamic contact angle measurement and tilting plate contact angle measurement.

- Sessile drop contact angle measurement, otherwise known as static angle measurement, is where a droplet of liquid is dropped onto a surface which is in the horizontal plane. As the droplet hits the surface it spreads out and this is used to measure the contact angle[69].

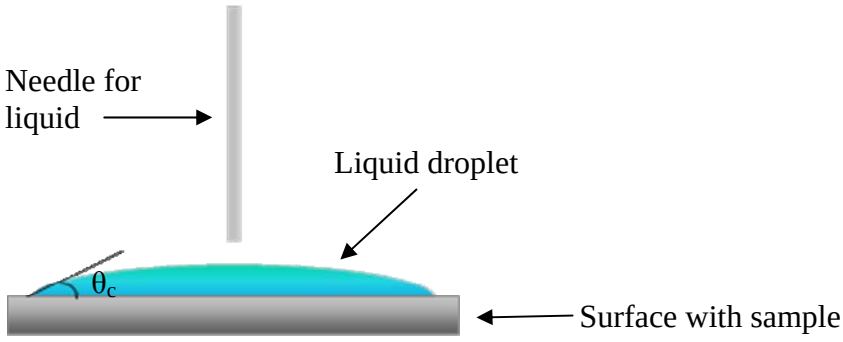

Figure 2.1 – Schematic representation of sessile drop contact angle measurements.

- Dynamic contact angle measurement: A droplet of liquid is placed on a horizontal sample. The volume of this droplet in then increased and decreased until equilibrium is reached between the three phases. As a direct result the three phase point across the sample surface increases. The advancing contact angle (θ_a) is determined as the volume of the droplet increases. The receding angle (θ_r) is determined as the volume of the droplet decreases. The difference between θ_a and θ_r is known as the contact angle hysteresis[69].

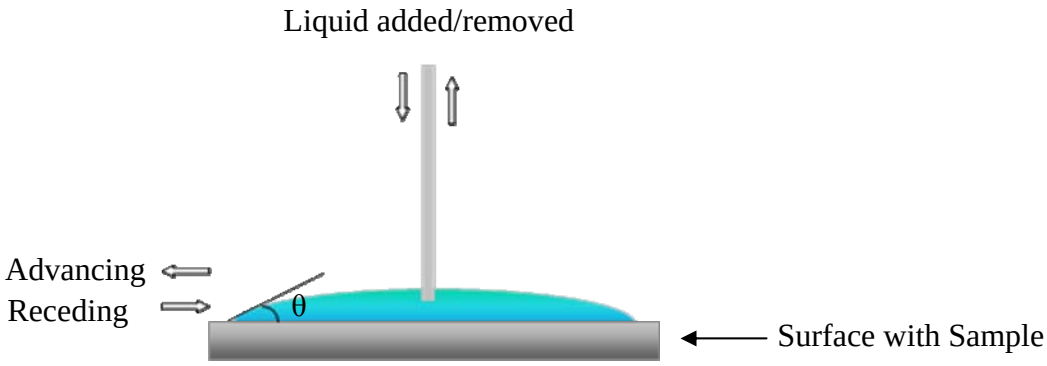

Figure 2.2 – Schematic representation of dynamic contact angle measurement.

- Tilting plate contact angle measurements: The θ_a and θ_r angles are measured as a droplet of liquid is placed on a surface which is tilted from the horizontal position. Measurements have to be taken before the droplet starts to move[69].

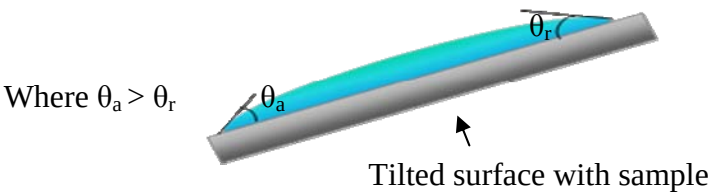

Figure 2.3 – Schematic representation of tilting plate contact angle measurements.

2.2 Ellipsometry

Ellipsometry is an optical non-destructive technique[70]. It uses polarised monochromatic light to determine the average thickness of a surface[7]. It works by monitoring the change in polarisation states after a beam is reflected from a surface of interest. A polarised light resolves into its parallel (s-polarised) and perpendicular (p-polarised) components after interacting with a surface at an angle. The resolved components are then compared to the incident light and the difference in amplitude and phase, with results in the thickness of the transition region between the reflective substrate and the air being determined[7] (**figure 2.4)**.

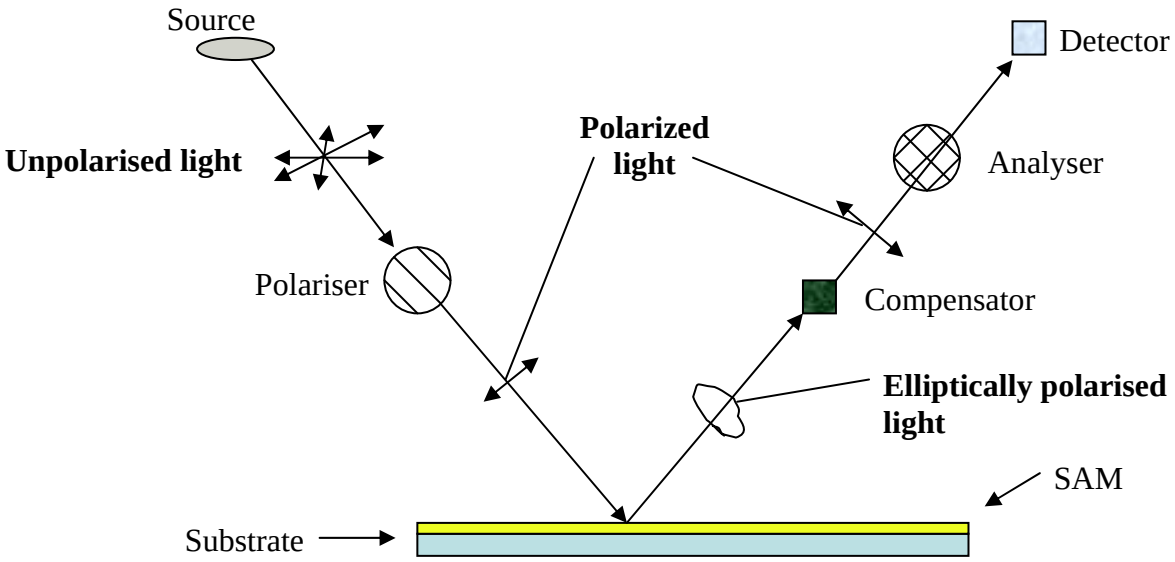

Figure 2.4 – Schematic description of an ellipsometer.

2.3 X-ray Photoelectron Spectroscopy

X-ray Photoelectron Spectroscopy (XPS) is a destructive technique which is widely used to investigate the chemical composition of surfaces[7].

XPS uses monochromatic x-rays to irradiate a sample. This is done in order to excite the core level electrons and is conducted under a vacuum[71]. When electrons have sufficient energy, the atom will emit an electron (**figure 2.5**) that is detected by the electron spectrometer and the kinetic energy of the emitted electron can be analyzed.

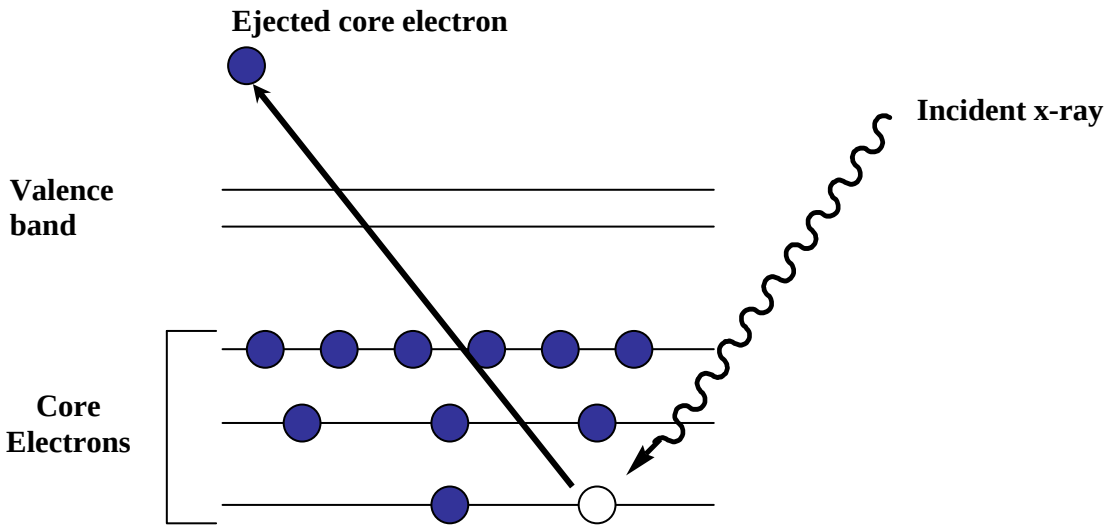

Figure 2.5 – Schematic diagram of the XPS process, showing the ejection of a core electron.

The binding energy of the electron released can then be calculated using the following equation[7];

$$E_B = hv - E_K - W$$

Where, E_B is the binding energy of the electron,
hv is the energy of the monochromatic x-ray,
E_K is the kinetic energy of the emitted electron
and W is the spectrometer work function.

All the quantities on the right hand side of the equation are either known or can be measured. Each element has a unique set of binding energies, Therefore the data calculated can be used to work out the elements present and the elemental composition of the SAM[7].

3.0 Project Overview

3.1 Hypothesis

This project involves fabricating an optimally spaced and well-defined SAM which eliminates the limitations highlighted in section 1.8 (page 16).

Figure 3.1 illustrates the main components involved in producing optimally spaced SAMs, where **1** is a thiol surfactant with a dialkylammonium ion centre, **2** is triethylene glycol thiol terminated alkane (TEGT), **3** is a crown ether coupled with any dendron and $\mathbf{G_1}$ is a first generation dendron.

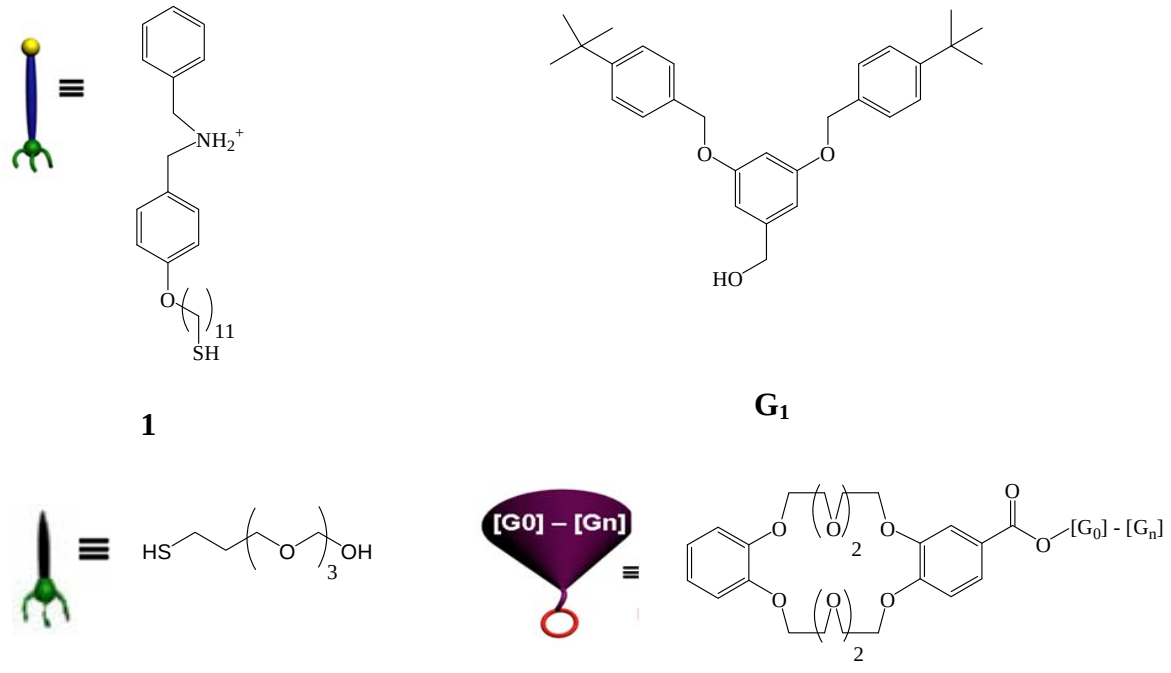

1 $\mathbf{G_1}$

2 **3**

Figure 3.1 – Main components involved in producing optimally spaced SAMs.

Scheme 3.1 illustrates how these components will be used to create optimally spaced and well-defined surfaces. A pseudorotaxane complex (**scheme 3.1, step 1**) will be formed in solution and the complex will be held together by hydrogen bonding[58].

The pseudorotaxane complexes will then be absorbed onto a Au surface *via* chemisorption in order to form a SAM (**scheme 3.1, step 2**). In this step the large steric bulk of the dendron controls the spatial separation of the chemisorbed moieties. Finally, the controlled release of DB24C8 with functionalised dendron from the surface, leaves behind spatially separated chemisorbed components. This is achieved by raising the pH of the solution resulting in the deprotonation of **3** causing the hydrogen bonding in the pseudorotaxane complex to be 'turned off'. Simultaneously, TEGT, **2**, will be used to fill the gaps created by the release of the crown, leaving an optimally spaced and well-defined surface (**scheme 3.1, step 3**).

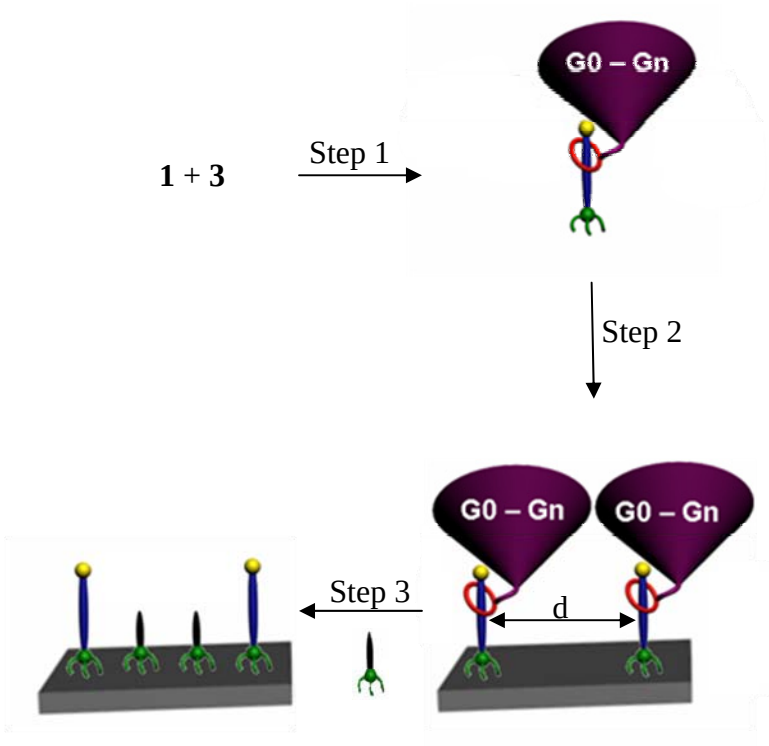

Scheme 3.1 – Proposed strategy for creating optimally spaced SAM, where d is a large spatial separation controlled by the size of a dendron.

3.2 Methodology

The project has been split into four main sections, (I) synthesis of crown ether covalently attached to a bulky dendron (**12**), (II) solution complexation studies, (III) SAM formation and (IV) control studies. Each of which are discussed below;

3.2.1 Synthesis of crown ether covalently attached to a bulky dendron

The first part of the project involves the synthesis of a crown ether covalently attached to a bulky dendron. There is a five step process to synthesise **12**, the first four steps are shown in **scheme 3.2** resulting in the formation of a crown ether with a functionalised acid. The acid **11** will then be coupled to a $\mathbf{G_1}$ to form a crown ether covalently attached to a bulky dendron (**Scheme 3.3**).

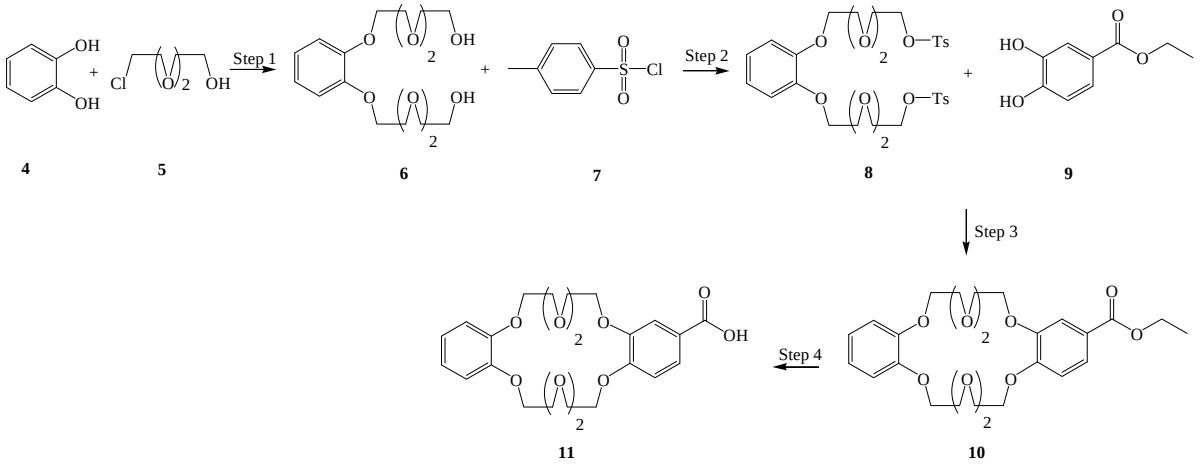

Scheme 3.2 – Overall synthesis of crown ether with functionalised acid.

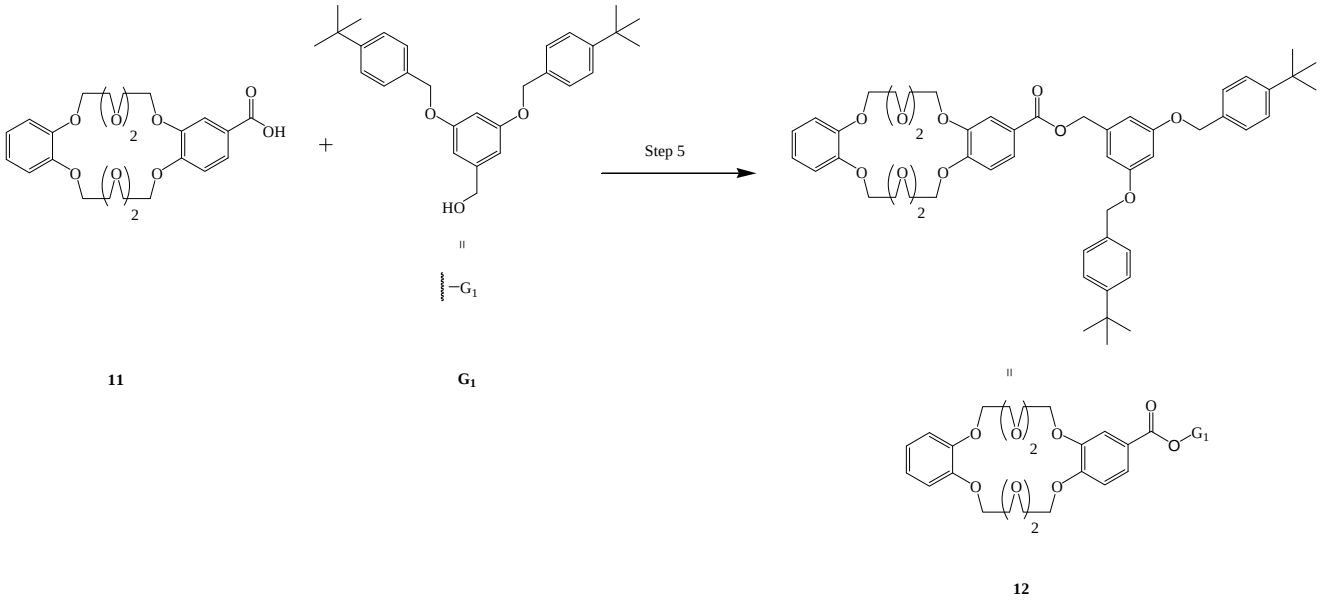

11 **G_1** **12**

Scheme 3.3 - Schematic for the coupling reaction between **11** and **G_1**.

3.2.2 Complexation

In this part of the project two complexation reactions were conducted between **1** and DB24C8 and **1** and **12** to form pseudorotaxane like species. **Scheme 3.4** shows the complexation between **1** and DB24C8.

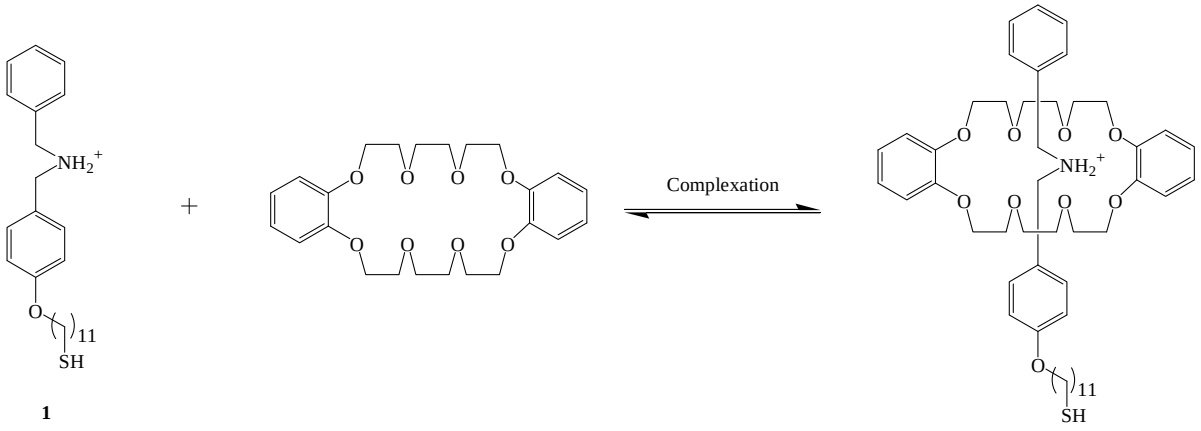

1

Scheme 3.4 - Schematic for the complexation between **1** and DB24C8 held together by hydrogen bonds from the NH_2^+ centre (donor) to the crown ether oxygen atoms (acceptors).

3.2.3 SAM Formation

The aim of the overall project is to create a mixed monolayer that was optimally spaced, which contained 2 different components. Before this can be done an understanding of the individual components is required. To do this, kinetic studies were carried out on the SAM formation of **2** (**Scheme 3.5a**) and **1** (**Scheme 3.5b**). SAM formation was monitored over a period of 24 hours and then characterised by contact angle, ellipsometry and XPS.

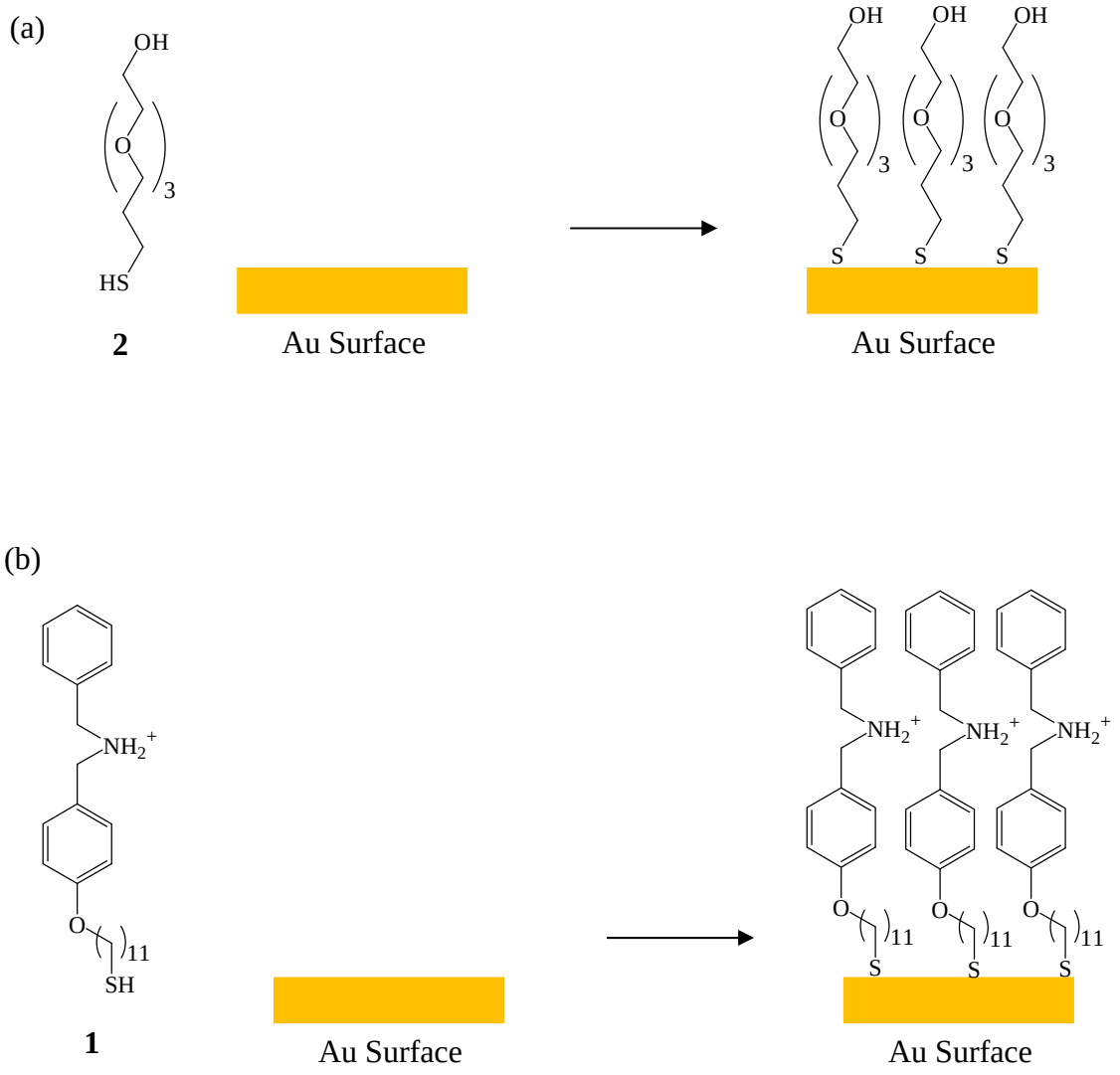

Scheme 3.5 – (a) SAM formation of **2** and (b) SAM formation of **1**.

3.2.4 Control Studies

There were two control studies that were carried out, these are discussed below;

(1) Control study 1 was designed to show that there is zero affinity between **12** and a clean gold surface. For this study a gold sample was immersed in a solution of **12** and compared to a gold sample immersed in a solution of ethanol. This study is crucial as it will tell us if excess **12** can be used in the complexation step with **1** (**Scheme 3.6**).

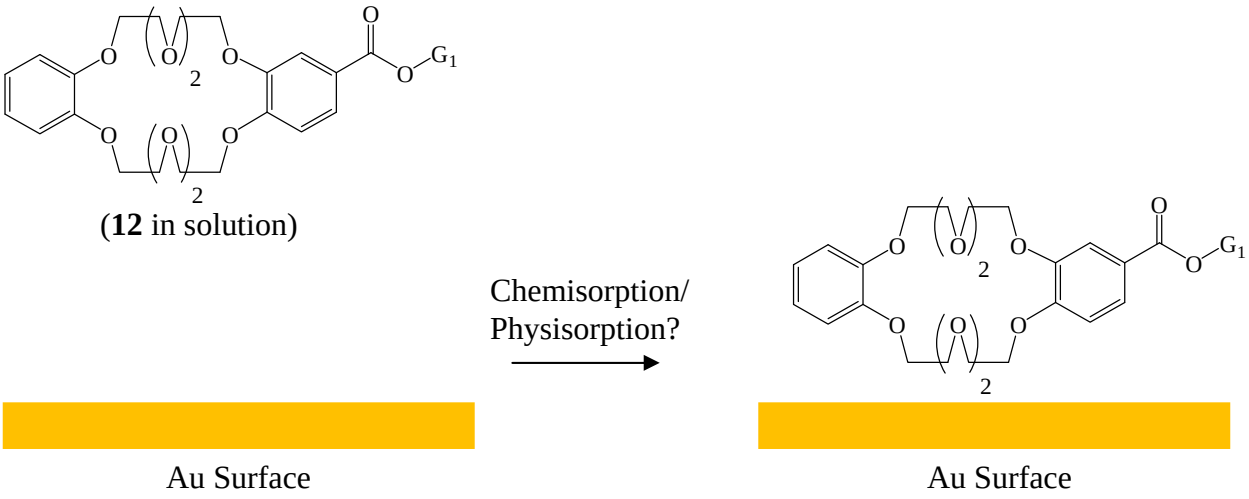

Scheme 3.6 – Control study 1

(2) Control study 2 is a displacement study. In this study a fully formed dialkylammonium thiol, **1**, SAM will be immersed in a solution of TEGT, **2**, (**Scheme 3.7**) for a period of 24 hours. The SAM will be characterised before and after immersion in the TEGT, **2**, solution. If both characterisations are similar we can assume that TEGT, **2**, does not displace the dialkylammonium thiol, **1**. However, if TEGT, **2**, does displace (**Scheme 3.7**) it will cause a problem when it is used to backfill the SAM, as the dialkylammonium thiol, **1,** needs to remain in its original position if optimally spaced SAMs are to be created.

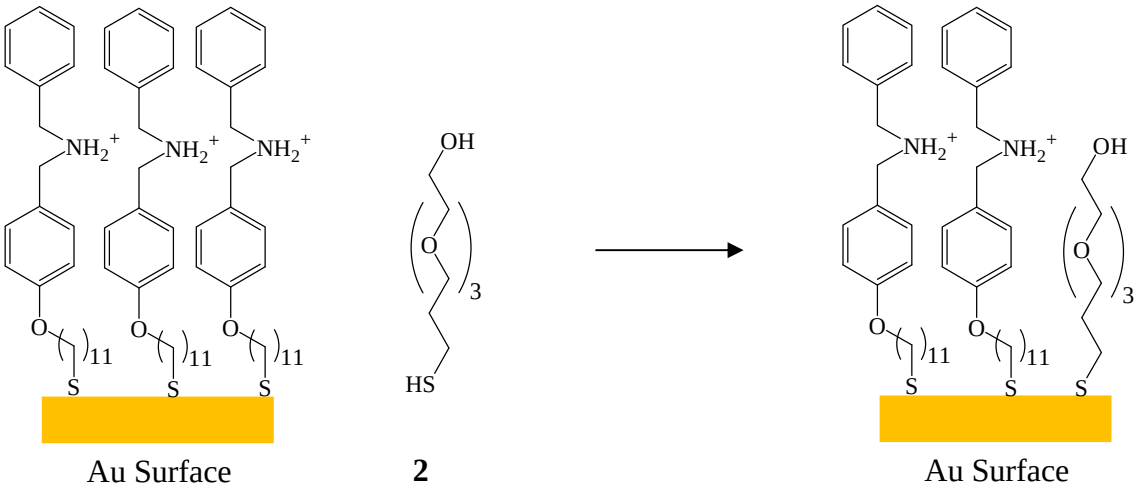

Scheme 3.7 – Displacement study.

4.0 Results and Discussion

4.1 Synthesis of crown ether covalently attached to a bulky dendron

The synthesis of **11** was conducted in 4 steps. Each of these steps were completed successfully and are discussed below.

Step 1 (**Scheme 3.2**)

Ether formation of **6** was successfully achieved by the employment of K_2CO_3 and KI. The reaction followed an S_N2 pathway and the mechanism is shown in **scheme 4.1**. **Scheme 4.1** shows monoalkylation of **4**. Ether glycol **5** was activated further by halogen exchange with KI, as this will increase the rate of reaction due to the C-I bond being weaker than the C-Cl bond. At the same time the carbonate base deprotonates **4**, to form the phenoxide **4'** which acts as the nucleophile and subsequently attacks the σ* (C-I) orbital of **5'** to generate the monosubstituted product. The same reaction occurs on the other hydroxyl group of **4** to afford **6**.

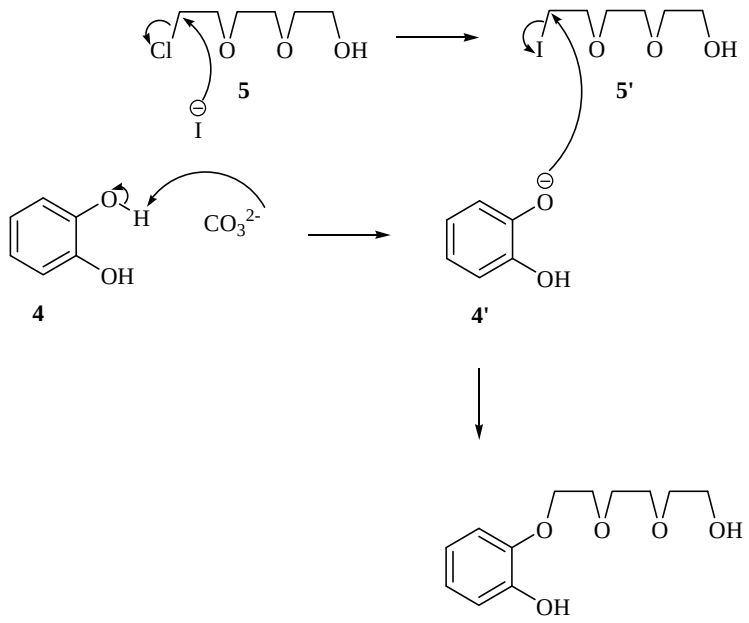

Scheme 4.1 – Mechanism for monoalkylation of **4**.

Step 2 **(Scheme 3.2)**

Formation of sulfonate ester **8** was successfully achieved by the employment of 4-dimethylaminopyridine (DMAP) and triethylamine (NEt_3). The reaction followed an S_N2 pathway and the mechanism is shown in **scheme 4.2**. **Scheme 4.2** shows monotoslyation of **6**. DMAP attacks the sulfur in **7** to form a highly reactive tosyl group **7'** *in situ*. The hydroxyl group on the nucleophile **6** attacks **7'** to regenerate the catalyst DMAP. Subsequently NEt_3 base deprotonates the intermediate to form the monotosylated product. The same reaction occurs on the other hydroxyl group of **6** to afford **8**.

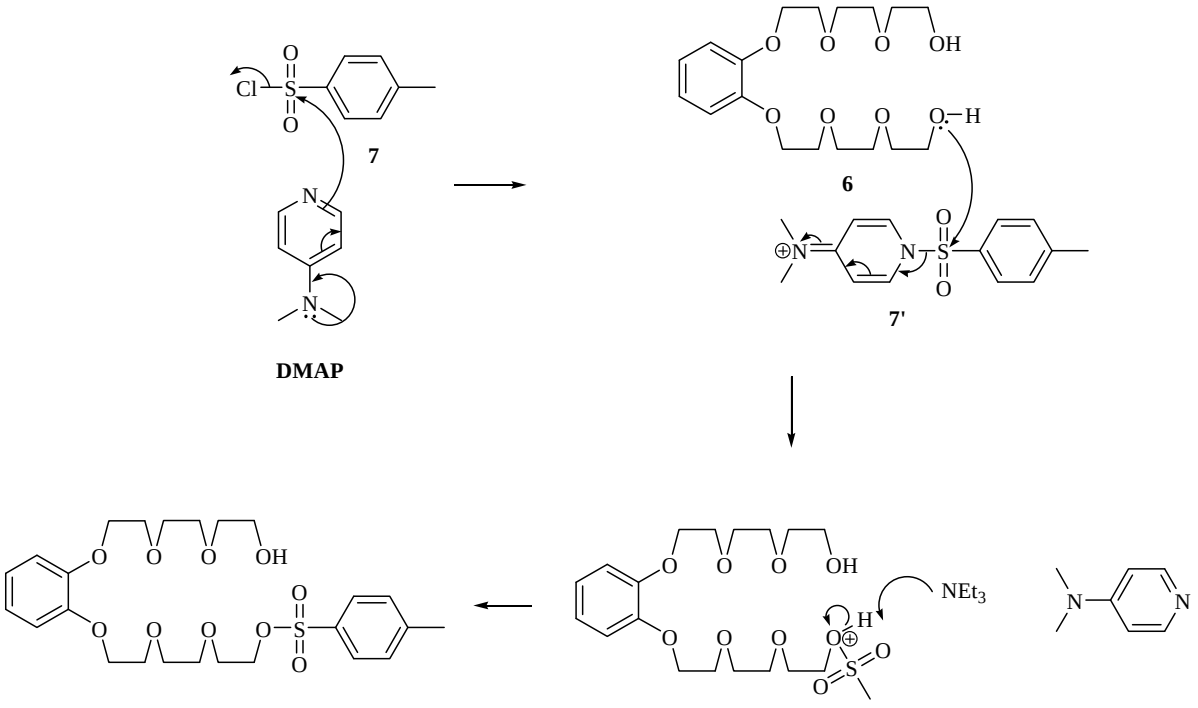

Figure 4.2 – Mechanism for monotosylation of **6**.

Step 3 **(Scheme 3.2)**

Ether formation of **10** was achieved by the employment of K_2CO_3 and lithium bromide (LiBr). The reaction proceeds *via* an S_N2 pathway and the mechanism is shown in **scheme 4.3**. **Scheme 4.3** shows the dialkylation of **9** resulting in the formation of a crown ether. Firstly, the carbonate base deprotonates both hydroxyl groups forming **9'**. This acts as a nucleophile and attacks the carbon adjacent to the tosyl group to form the ether **8'**. The K^+ ion coordinates to the lone pair of electrons on the terminal oxygens in the glycol ether chain. This places glycol ether chains in close enough proximity for the reaction to continue. In the second part of the reaction the deprotonated hydroxyl group on **9'** acts as a nucleophile and attacks the carbon adjacent to the tosyl group, resulting in ring closure and the formation of a crown ether **10**. During the reaction mechanism the LiBr scavenges the protons released during the deprotonation of **9**.

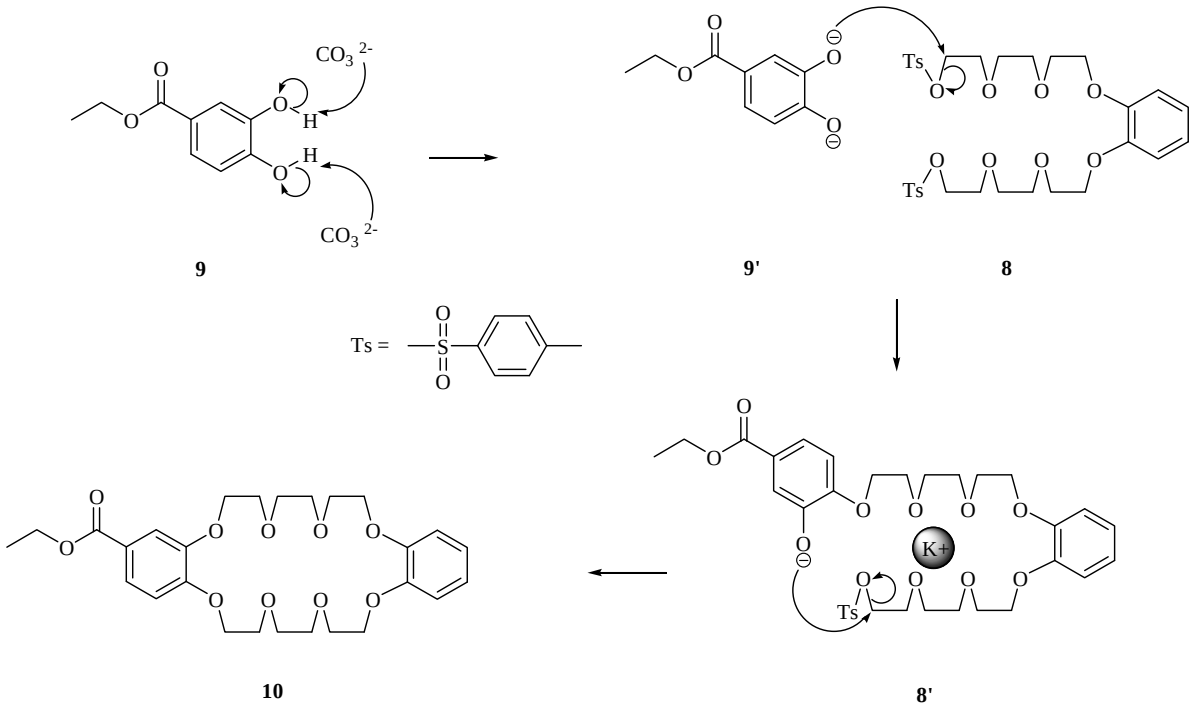

Scheme 4.3 – Mechanism for dialkylation of **9**.

Figure 4.1a shows the ^{1}H NMR for **10**. It indicates the presence of an ethyl ester as both the methyl (Ha) and methylene (Hb) are observed.

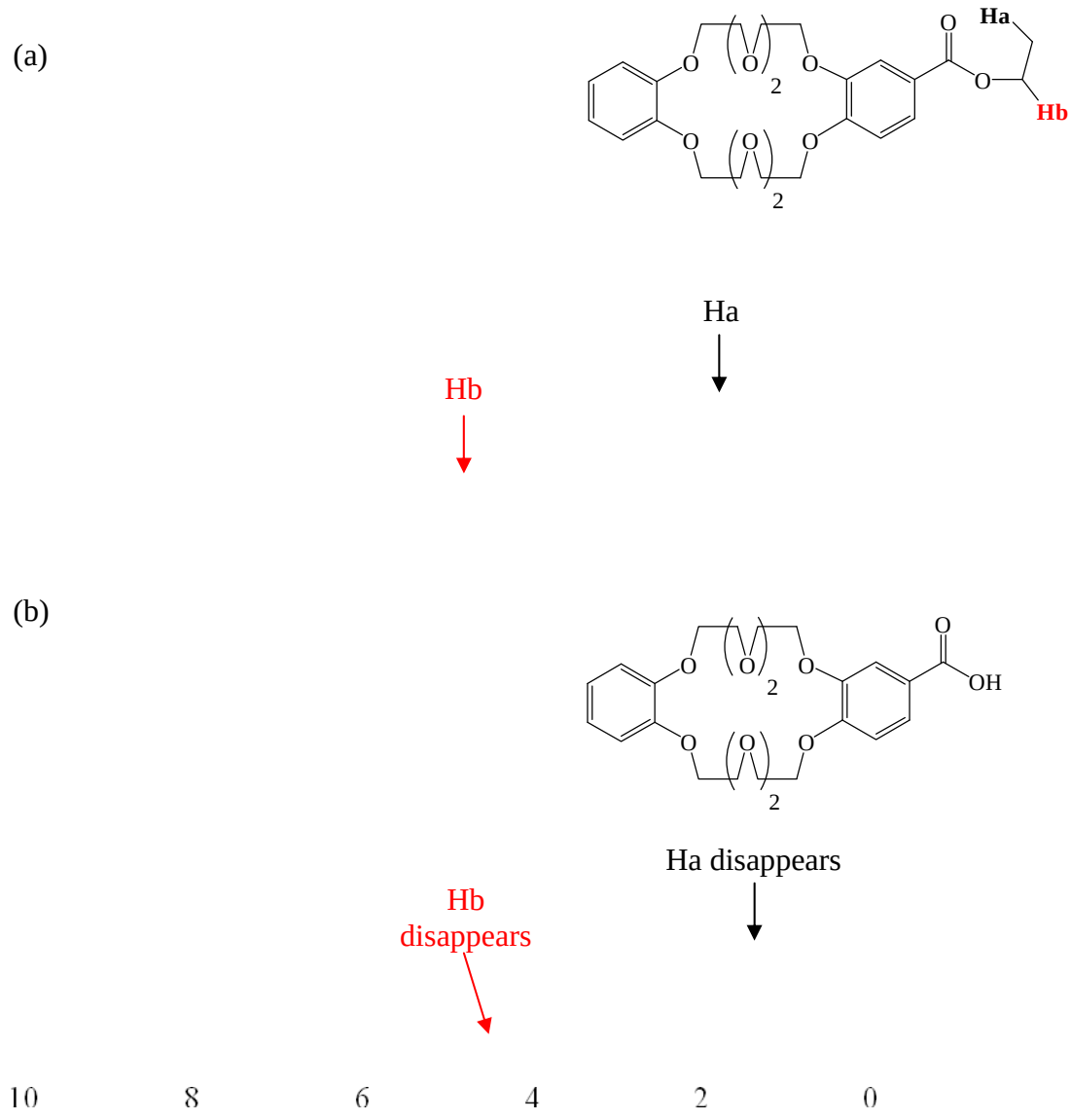

Figure 4.1 – (a) ^{1}H NMR of **10** and (b) ^{1}H NMR of **11**.

Step 4 **(Scheme 3.2)**

Formation of an acid **11** was facilitated by the employment of KOH. The reaction proceeds *via* tetrahedral intermediate (**scheme 4.5**) under basic conditions. Initially the base attacks the δ^+ carbonyl to form the tetrahedral intermediate **10'**. The negative charge then rehybridises around the tetrahedral intermediate to expel the ethoxy group. This is expelled with a negative charge, which then deprotonates the acid **10''**, forming the carboxylate anion **10'''**. Upon acidification the carboxylate anion **10'''** is protonated forming the desired acid **11.**

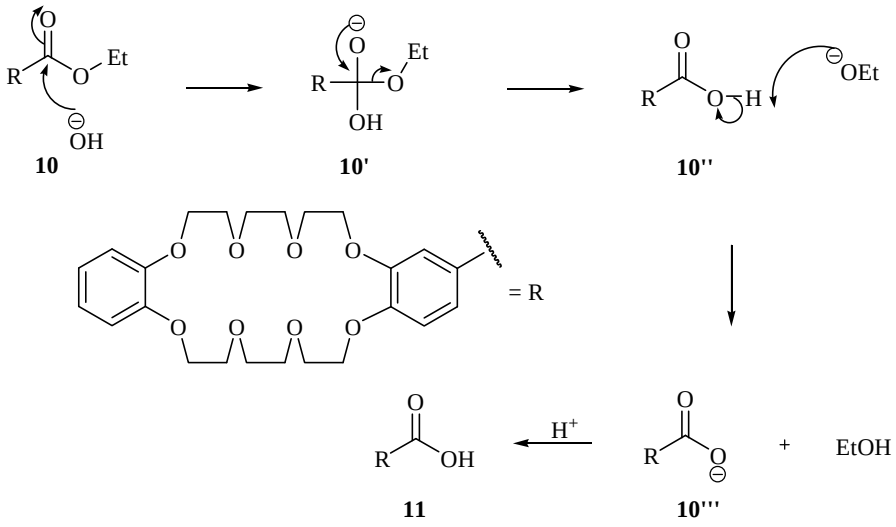

Scheme 4.5 – Mechanism for the hydrolysis of **10**.

Figure 4.1b shows the ^{1}H NMR after ester **10** was successfully hydrolysed. The success of the transformation can be seen in **figure 4.1b**, where both Ha and Hb ^{1}H signals disappear, showing that the ethyl group has been cleaved.

Step 5 **(Scheme 3.3)**

Ester formation of **12** was successfully achieved by the employment of dicylohexylcarbodiimide (DCC) as a dehydrating agent. The mechanism for this is shown in **scheme 4.6**. During this process dicyclohexylurea (DHU) is produced as a bi product. Initially the DCC acts as a base and deprotonates the acid **11.** The protonated form of DCC is susceptible to nucleophilic attack from the carboxylate anion *via* the carbon centre forming the imine **11'**. **11'** is protonated allowing **12** to act as a nucleophile which attacks the carbonyl carbon. As a result the urea side product DHU is released and the protonated ester is neutralised to give **12**.

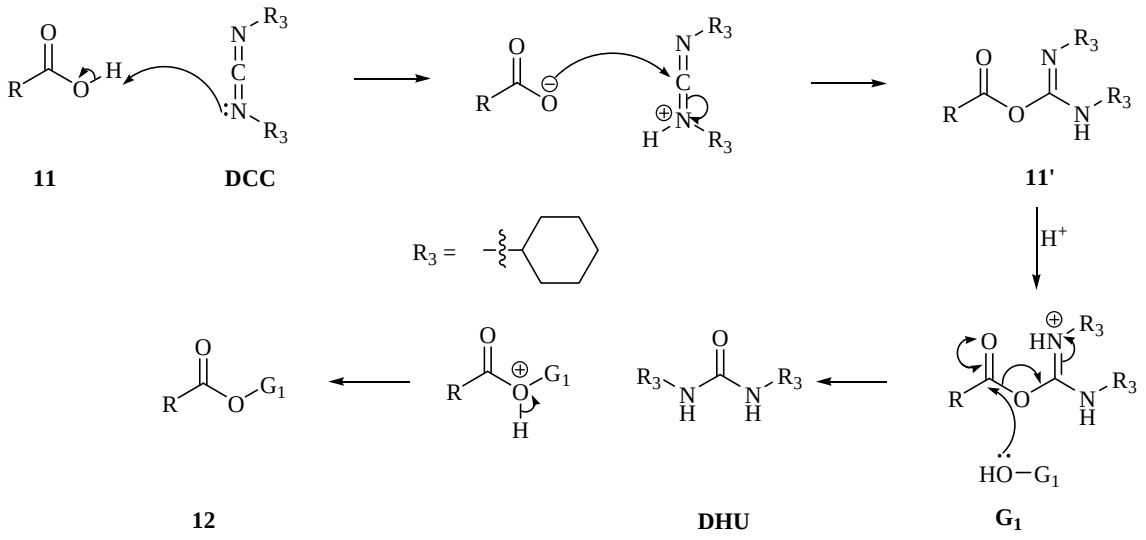

Scheme 4.6 – Mechanism for the ester formation of **12**.

4.2 Complexation Studies

In this project two complexation reactions were conducted, these are discussed below;

Complexation 1

In the first complexation study, we tried to complex DB24C8 with **1** to form a pseudorotaxane like complex. The ^{1}H NMR spectra (**figure 4.2a**) of **1** shows Hc at δ = 4ppm, whereas the ^{1}H NMR spectra (**figure 4.2b**) of a 1:1 mixture of DB24C8 and **1** shows Hc at δ

= ~4.5ppm. The chemical shift relates to a pseudorotaxane complex being formed between the dialkylammonium centre (NH_2^+) and the DB24C8. This is the same chemical shift that is observed in the literature[72]. The complex is held together by N^+-H---O and C-H---O hydrogen bonds. Integration of the spectra indicated that some of the starting materials (dialkylammonium thiol, **1**, and DB24C8) were still present. This is expected as the reaction is in equilibrium. This could cause problems when attempting to attach the complex to a gold surface, as any uncomplexed dialkylammonium thiol, **1**, will still bind to the surface. Therefore further work is required in the complexation step before SAM formation can take place.

(a)

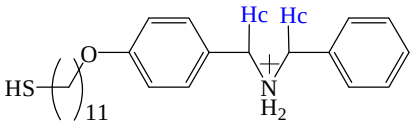

(b)

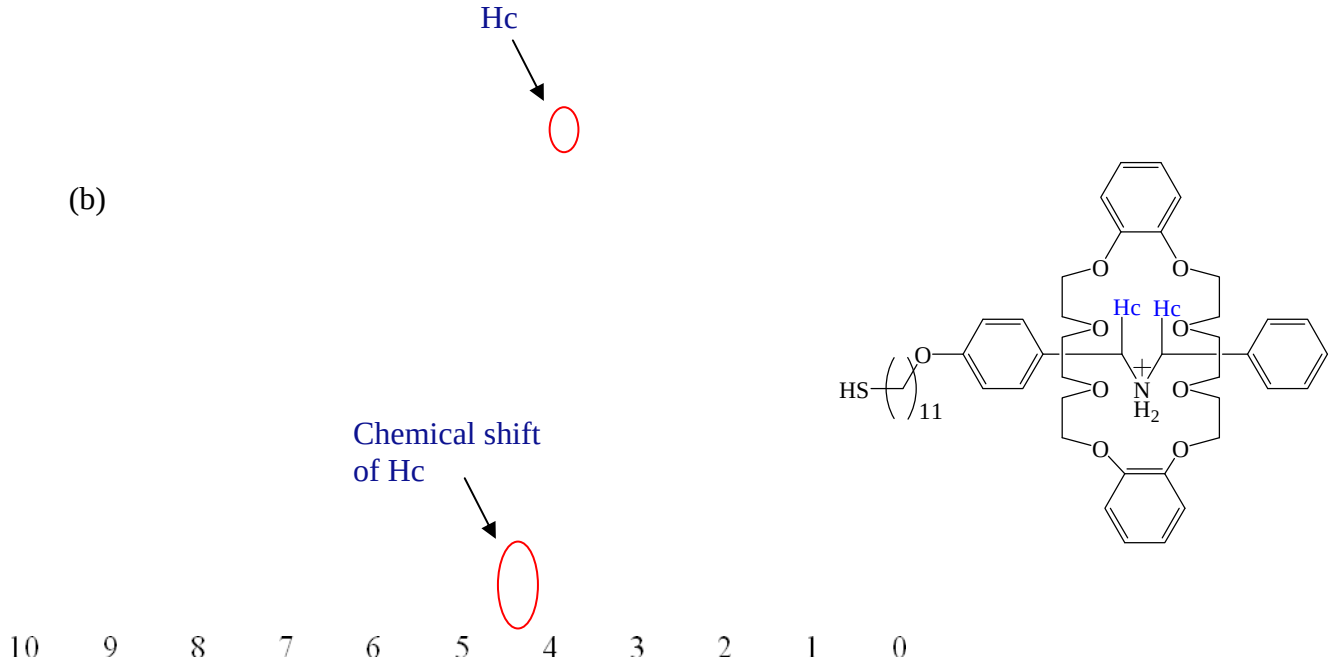

Figure 4.2 – (a) H NMR of **1** and (b) ^{1}H NMR of 1:1 mixture of DB24C8 and **1**.

Complexation 2

In the second complexation study, we tried to complex compound **12** with **1** to form a pseudorotaxane like complex. The ^{1}H NMR spectra (**figure 4.2a**) of **1** shows Hc at δ = 4ppm, whereas the ^{1}H NMR spectra (**figure 4.3**) of a 1:1 mixture of **12** and **1** shows Hc at δ = ~4.5ppm. The chemical shift relates to a pseudorotaxane complex being formed between the dialkylammonium centre (NH_2^+) and the crown in **12**. This is the same chemical shift that is observed in the literature[72]. The complex is held together by N^+-H---O and C-H---O hydrogen bonds. Integration of the spectra indicated that some of the starting materials (dialkylammonium thiol, **1**, and **12**) were still present. This is expected as the reaction is in equilibrium. This could cause problems when attempting to attach the complex to a gold surface, as any uncomplexed dialkylammonium thiol, **1**, will still bind to the surface. Therefore further work is required in the complexation step before SAM formation can take place.

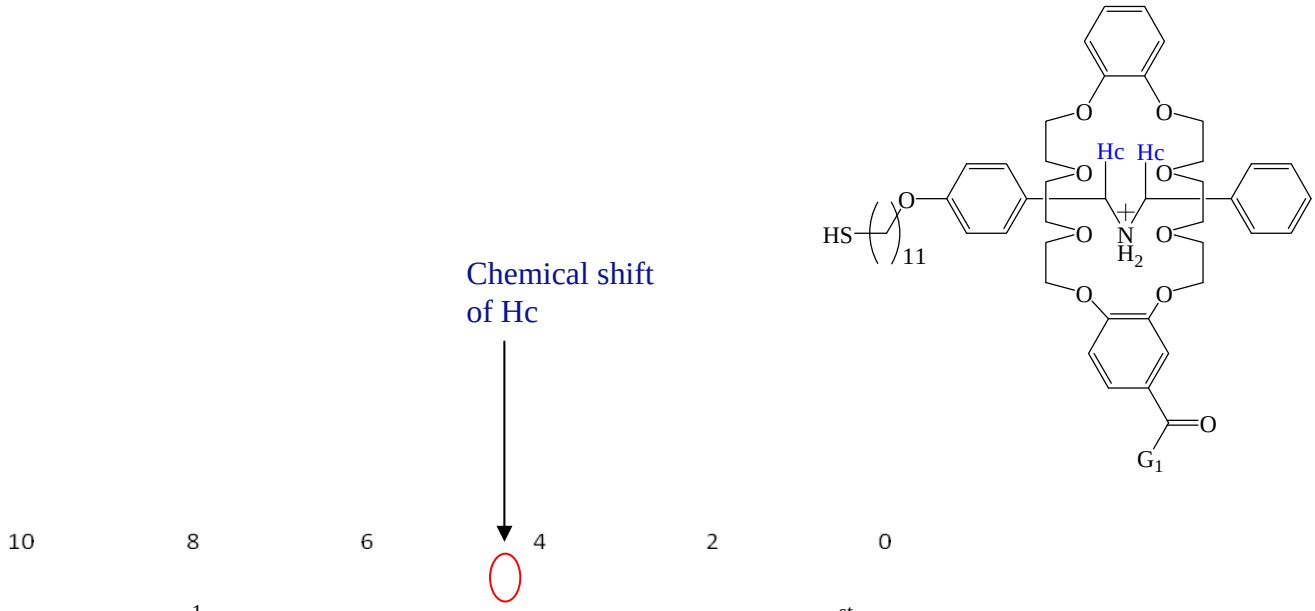

Figure 4.3 – ^{1}H NMR of 1:1 mixture of **12** and **1**, where $\mathbf{G_1}$ = 1st generation dendron.

4.3 SAM Formation

4.3.1 Formation of TEGT SAM (Scheme 3.5a)

This study was a kinetic study designed to work out the optimal time to create a well packed TEGT, **2**, monolayer. The SAMs were made at different time intervals (2hr, 4hr, 8hr, 16hr and 24hr) and then characterised by contact angle and ellipsometry, with the 24hr SAM also being characterised by XPS.

Contact angle

Figure 4.4 shows the advancing and receding angles for all time intervals.

The TEGT, **2**, SAM has a hydroxyl end group therefore the surface is expected to be hydrophilic as there will be interactions between the water droplet and the monolayer[7]. Hence a low contact angle should be observed[7].

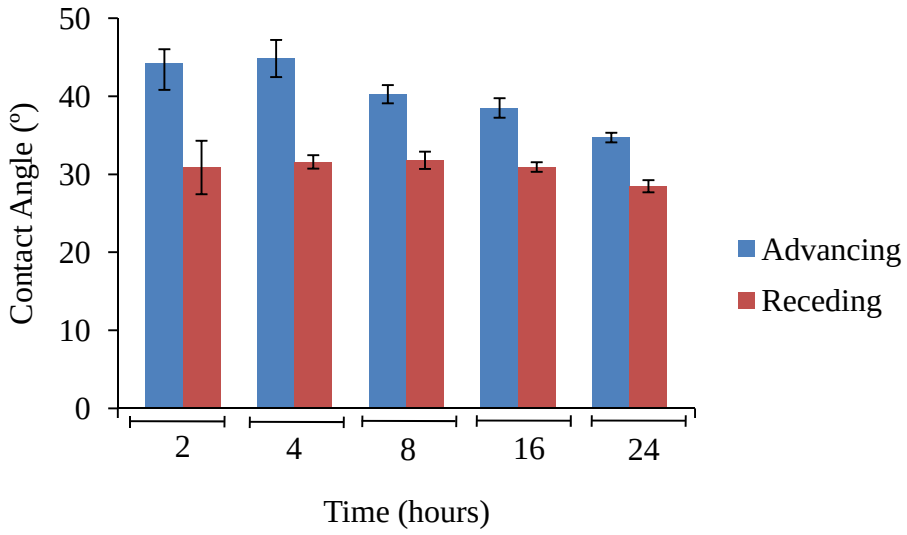

Figure 4.4 – Advancing (θ_a) and receding (θ_r) contact angle data for SAM formation of TEGT, **2**.

Figure 4.4 shows that after 24 hours the advancing and receding angle are at their lowest (34.7° θ_a, 28.5° θ_r), suggesting that the monolayer is more hydrophilic than at the 2 hour time point. Following chemisorption at 2 hours, intermolecular interactions can occur between neighbouring backbones of the surfactant molecules causing molecular ordering and the

formation of a more densely packed monolayer. The hydrophilic end groups of the surfactant are therefore in closer proximity to one another, which results in a more hydrophilic surface being detected by contact angle.

Throughout the 24 hour time period the hysteresis of the angle is decreasing. At 2 hours the hysteresis was 14º whereas at 24 hours the hysteresis is 6º. Previous studies[7] have shown that the hysteresis is affected by the roughness of the surface or the molecular ordering of a surface. As the gold samples were all cut from the same supply we can assume that the difference in hysteresis is caused by the molecular ordering.

The literature[74-76] shows a range of advancing angles (42º-38º) and receding angle (33º-24º) for an ethylene glycol terminated SAM. The experimental data obtained are comparable with the range shown in the literature, thus indicating that an ethylene glycol SAM has been formed.

Ellipsometry

Table 4.1 shows the ellipsometry data collected for all samples collected this can then be compared to the Chem Draw (ultra 3d 8.0) prediction for the length of the molecule (1.663nm). From these figures, it suggests that a single monolayer has been formed instead of a bilayer as the average thickness is less than predicted. The difference may be attributed to the monolayer forming at a tilt from the Au surface.

Table 4.1 – Ellipsometry data for SAM formation of **2**.

Time (hours)	Average Thickness (nm)	Standard Error (nm)
2	0.452	0.123
4	0.449	0.153
8	0.637	0.165
16	0.589	0.173
24	0.734	0.167

X-ray Photoelectron Spectroscopy (XPS)

For the purposes of this study, the element we were most interested in analysing was sulfur. **Figure 4.5a** shows the sulfur binding energy spectra for a TEGT SAM formed after 24 hours of immersion. The sulfur XPS spectrum revealed the characteristic S2p3/2 and S2p1/2 doublet with components at 162.1 and 163.9eV, indicative of a thiolate bound to a gold surface[77]. When compared to **figure 4.5c** (bare gold) it clearly shows that formation of a Au-S bond has taken place indicating TEGT, **2**, SAM formation.

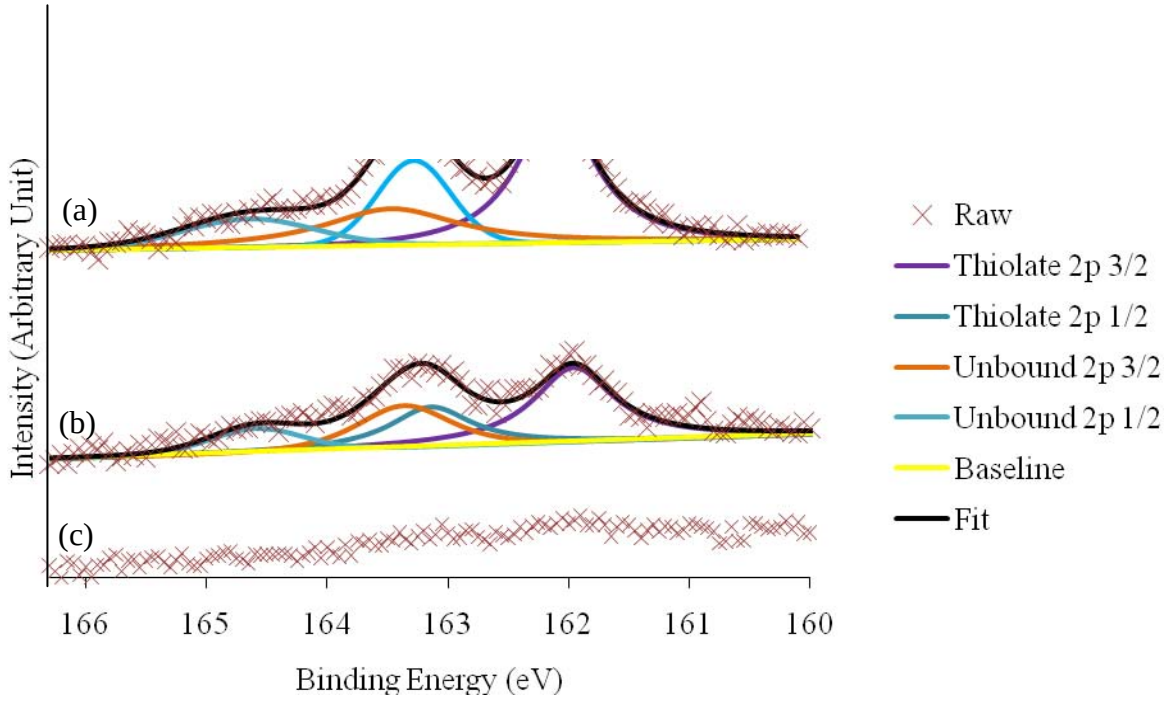

Figure 4.5 – XPS data for sulphur peaks of (a) TEGT (**2**), (b) dialkylammonium thiol (**1**) and (c) bare gold

However, the XPS data also indicated some unbound thiol on the surface. The detection of the S-H bond shows that some of the TEGT, **2,** molecule is only physisorbed to the surface, not chemically bonded. It is possible to decrease the amount of unbound TEGT, **2**, on the surface by improving the cleaning procedure once SAM formation has taken place.

Overall the three characterisations indicate that SAM formation of a single monolayer has taken place over all time frames, but if left for 24 hours, higher molecular ordering is achieved.

4.3.2 Formation of a dialkylammonium thiol SAM (Scheme 3.5b)

This study was a kinetic study designed to work out the optimal time to create a well packed dialkylammonium thiol, **1**, monolayer. The SAMs were made at different time intervals (2hr, 4hr, 8hr, 16hr and 24hr) and then characterized by contact angle and ellipsometry, with the 24hr SAM also being characterized by XPS.

Contact angle

Figure 4.6 shows the advancing and receding angles for all time intervals. The dialkylammonium thiol, **1**, is phenyl terminated, therefore you would expect it to be more hydrophobic than TEGT[7].

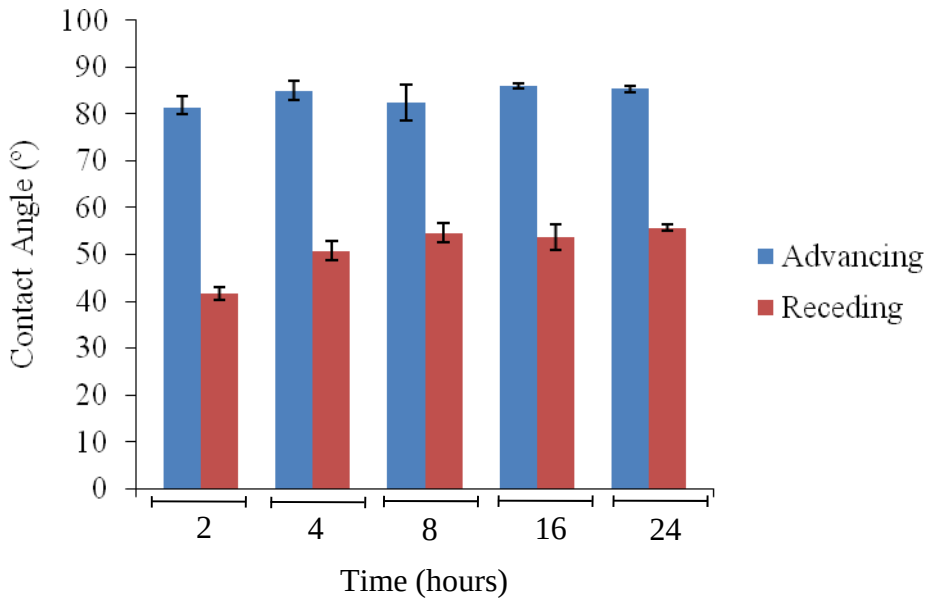

Figure 4.6 – Advancing (θ_a) and receding (θ_r) contact angle data for SAM formation of dialkylammonium thiol, **1**.

Figure 4.6 shows that throughout the 24 hour time period the advancing and receding angle remain similar, but the hysteresis does decrease over time from 35º (2hr) – 30º (24hr). The slight decrease in hysteresis indicates that some molecular ordering is occurring over time. The presence of the positively charged dialkylammonium ion can cause repulsion between surfactant molecules which will have effect on the packing of the monolayer and could explain the large (30º) hysteresis value.

Ellipsometry

Table 4.2 shows the ellipsometry data collected for all samples. The data can be compared to the Chem Draw (ultra 3d 8.0) prediction for the length of the molecule (2.898nm). From these figures, it suggests that a single monolayer has been formed rather than a bilayer as the average thickness is less than predicted for all time frames. The figures show a major change in the average thickness from 2 hours (1.889 nm) to 24 hours (2.856 nm). The difference could be due to a change in the molecular ordering of the SAM over the 24 hour time period. If molecular ordering is increasing the backbones of the surfactant molecule will be coming

into closer proximity which would cause an increase in the average thickness. These results also agree with the contact angle data suggesting that molecular ordering is increasing over the 24 hour time period.

Table 4.2 – Ellipsometry data for SAM formation of **1**.

Time (hours)	Average Thickness (nm)	Standard Error (nm)
2	1.889	0.252
4	1.829	0.256
8	2.37	0.388
16	2.197	0.492
24	2.856	0.385

XPS

For the purposes of this study, the element we were most interested in analysing was sulfur. **Figure 4.5b** shows the sulfur binding energy spectra for a dialkylammonium thiol, **1**, SAM formed after 24 hours of immersion. The sulfur XPS spectrum revealed the characteristic S2p3/2 and S2p1/2 doublet with components at 161.9 and 163.7eV, indicative of a thiolate bound to a gold surface[77]. When compared to **figure 4.5c** it clearly shows that formation of a Au-S bond has taken place indicating the formation of the dialkylammonium thiol, **1**, SAM. However, the XPS data also indicated some unbound thiol on the surface. The detection of the S-H bond shows that some of the dialkylammonium thiol, **1**, molecule is only physisorbed to the surface, not chemically bonded. It is possible to decrease the amount of unbound dialkylammonium thiol, **1**, on the surface by improving the cleaning procedure once SAM formation has taken place.

Overall the three characterisations show that SAM formation of a single monolayer has taken place over all time frames, but if left for 24 hours, higher molecular ordering is achieved.

4.4 Control studies

4.4.1 Control study 1 (Scheme 3.6)

This study was designed to show that there was no affinity between **12** and a clean gold substrate. Clean gold substrates were immersed in a 1mM solution of **12** in HPLC ethanol for a period of 24 hours and compared to gold substrates that were immersed in pure HPLC ethanol for 24 hours. After 24 hours, samples were compared *via* ellipsometry. **Table 4.3** shows the data collected. Ideally you would expect to obtain a thickness of 0nm, which would prove no affinity. However, **table 4.3** indicates that after 24 hour immersion the average thickness of both samples were ~ 0.5nm. These results are comparable, indicating that there is no major affinity of **12** with gold. The thickness that is shown to be present on the surface can be attributed to contaminants from the atmosphere.

Table 4.3 – Ellipsometry data for control study 1.

Sample	Average Thickness (nm)	Standard Error (nm)
EtOH	0.524	0.136
Compound **12**	0.541	0.149

To confirm these findings XPS will be required to show that there is no elements bound to the surface.

4.4.2 Control Study 2 (Scheme 3.7)

In this displacement study a formed dialkylammonium thiol, **1**, SAM was immersed in a 0.1mM solution of TEGT, **2**, for a period of 24 hours and then characterised by contact angle and ellipsometry. **Figure 4.7** shows the contact angle measurements (both θ_a and θ_r) for a fully formed dialkylammonium thiol, **1**, SAM before and after immersion into a solution of

TEGT for 24 hours. **Table 4.4** shows the ellipsometry data for a fully formed dialkylammonium thiol, **1**, SAM before and after immersion into a solution of TEGT, **2**, for 24 hours.

Contact angle

Figure 4.7 shows that after the dialkylammonium thiol, **1**, SAM was immersed in a solution of TEGT, **2**, the receding angle decreased to 33º. However, the advancing angle remained similar resulting in an increase of the contact angle hysteresis from ~30º to ~50º. This increase could be a direct result of a two component SAM being formed between the dialkylammonium thiol, **1**, and TEGT, **2**.

From the contact angle data it is not clear if the TEGT, **2**, has displaced the dialkylammonium thiol, **1**, or if it has simply filled in the space created by the existing repulsion between neighbouring backbones.

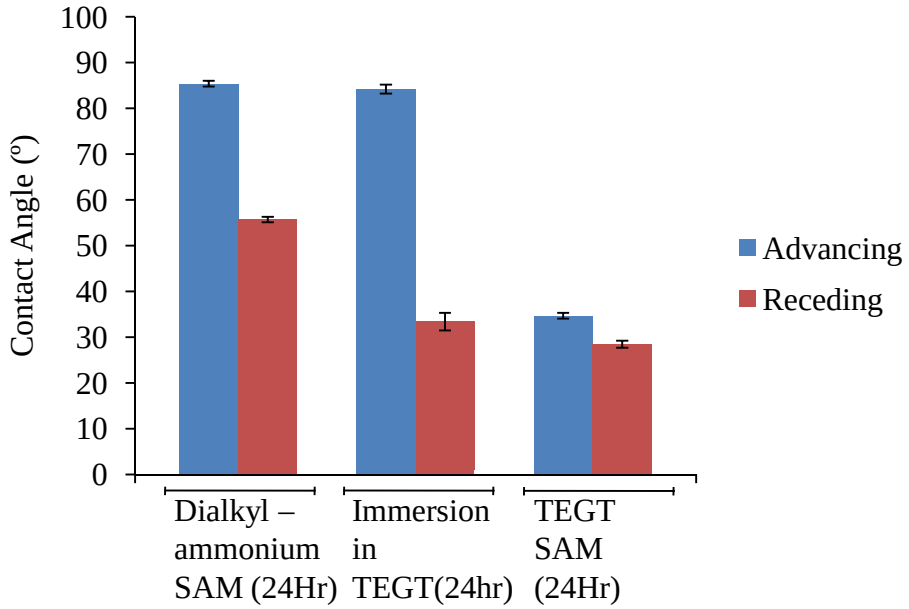

Figure 4.7 – Advancing (θ_a) and receding (θ_r) contact angle data for control study 2.

Ellipsometry

If there was relatively no change in the average thickness (**table 4.4**) we could say that the TEGT, **2**, does not displace the dialkylammonium thiol, **1**. However, **table 4.4** shows that after a fully formed dialkylammonium thiol, **1**, SAM was immersed in TEGT, **2**, for 24 hours, a decrease in the average thickness of the SAM was observed. This observation could be attributed to displacement of the dialkylammonium thiol, **1**, molecules (molecular length ~ 3.0 nm) by the shorter TEGT, **2**, molecules (molecular length ~1.7 nm).

From this control study we were unable to determine the level of displacement. For full displacement to have taken place the average thickness should have been similar to that shown in control study 2 (0.734nm).

Table 4.4 – Ellipsometry data for control study 2.

SAM	Average Thickness (nm)	Standard Error (nm)
Dialkylammonium thiol (**1**)	2.856	0.385
After 24Hr immersion in TEGT (**2**)	1.832	0.314

Contact angle and ellipsometry suggest that TEGT, **2**, partially displaces the dialkylammonium thiol, **1**, from the SAM. However, XPS can be used to confirm this as TEGT, **2**, contains no nitrogen (N) atoms therefore the reduction in the N: S ratio will indicate displacement having taken place.

5.0 Conclusion

The overall goal of the research, as shown in **scheme 3.1** was divided into three steps. Before these could be attempted the synthesis of a crown ether covalently attached to a bulky dendron, **12** (**Scheme 3.3**) was required. This was achieved successfully over a five step synthesis. Each step provided relatively good yields when compared to that obtained in the literature[72, 73]. The success of this five step synthesis allowed the complexation step (**Scheme 3.1, step 1**) to begin.

Both complexation studies (between DB24C8 and **1** and **12** and **1)** were shown to be successful as the ^{1}H NMR indicated the relevant chemical shift[78] and that the process was in equilibrium.

Before the second part of the research (**Scheme 3.1, step 2**) could be conducted the single components involved (dialkylammonium thiol, **1**, and TEGT, **2**) were studied and are concluded below.

SAM formation of a single monolayer of dialkylammonium thiol, **1**, was achieved successfully for all time frames (2-24 hours). Surface characterisations did reveal that for higher molecular ordering the immersion time had to be at least 24 hours, as the contact angle hysteresis decreased with time.

SAM formation of a single monolayer of TEGT, **2**, was achieved successfully for all time frames (2-24 hours). Contact angle measurements indicated that higher molecular ordering was achieved after TEGT was immersed for a period of 24 hours, as the contact angle hysteresis decreased with time.

During the research project two control studies were carried out:

(i) Control study 1 gave a first indication that there was no major affinity between **12** and Au surface concluding that the use of excess **12** will have no major effect on SAM formation when the complexes are applied to a Au surface.

(ii) Control study 2 highlighted that after a formed dialkylammonium thiol, **1**, SAM was immersed in TEGT, **2**, for 24 hours the physical properties of the newly formed SAM had changed. The ellipsometry data indicates that this could have been caused by the TEGT, **2**, displacing the dialkylammonium thiol, **1**. However the extent of the displacement is unknown.

6.0 Future work

1. XPS should be carried out on both control studies to confirm (a) **12** has no affinity to a Au surface and (b) TEGT does displace the dialkylammonium thiol.

2. If findings confirm that TEGT does displace the dialkylammonium thiol, further control studies are required to determine to what extent TEGT displaces a dialkylammonium thiol SAM. A proposed study would involve creating a dialkylammonium SAM and then immersing it in a solution of TEGT for various time frames (2hr, 4hr, 8hr, 16hr and 24hr). After surface characterisation, it would be possible to determine how long it will take a TEGT molecule to displace a fully formed dialkylammonium SAM.

3. If TEGT displaces at all time intervals, the head group of the dialkylammonium thiol could be altered to a thioctic acid group which has been found[78] to form a stronger bond with a Au surface when compared to S-Au bond.

4. Once XPS confirms that **12** has no affinity to Au, both complexation steps should be repeated using an excess of crown ether. This should be done to maximise the complexation of dialkylammonium thiol which will limit the amount of free dialkylammonium thiol binding to the Au surface during SAM formation.

5. Once the complexation steps have been optimised the pseudorotaxane like complex will be absorbed onto a surface *via* chemisorption (**Scheme 3.1, step 2**). In this step the large steric bulk of the dendron controls the spatial separation of the chemisorbed moieties. After which, the control release of the crown covalently attached to a bulky

dendron, will be achieved by raising the pH of the solution resulting in the deprotonation of the dialkylammonium thiol causing the noncovalent interaction in the pseudorotaxane complex to be ‘turned off’. Simultaneously TEGT, **2**, will be used to fill the gaps created by the release of crown ether with functionalised dendron (**Scheme 3.1, step 3**). Thus creating an optimally spaced and well defined surface.

7.0Experimental

7.1 General Procedure

The commercially available chemicals were purchased from either Sigma Aldrich (Dorset, United Kingdom) or Fisher (Loughborough, United Kingdom). Compound **1** (**figure 3.1**) and **2** (**figure 3.1**) were synthesised by Dr Parvez Iqbal. Thin layer chromatography (TLC) was carried out on aluminium plates coated with silica gel 60 F_{254} (Merck 5554). The TLC plates were air dried and viewed under a UV lamp (254nm) or developed in permanganate solution and heat dried. Column chromatographic separations were performed using silica gel 120 (ICN Chrom 32- 63, 60Å) Compounds were then characterised by ^{1}H Nuclear Magnetic Resonance (NMR), ^{13}C NMR and mass spectrometry.

7.2 Spectroscopic analysis

^{1}H NMR spectra were recorded using a Brucker AC 300 spectrometer.^{13}C NMR spectra were recorded on a Brucker AV 400 (100MHz) using a pendent pulse sequence. Chemical shifts are quoted in ppm to higher frequency from $SiMe_4$ using deuterated chloroform as the lock and the residual solvent as the internal standard. The coupling constants are shown in Hertz (Hz) with multiplicities abbreviated as follows; s = singlet, d = doublet, dd = double doublet, t = triplet, q = quartet and m = multiplet. Mass spectrometry was carried out by electron impact (EI) mass spectrometry; performed on VG Prospec and electrospray mass spectroscopy (ES); performed on a micromass time of flight (TOF) using methanol as the mobile phase.

7.3 Synthesis

Synthesis of compound 6[72]

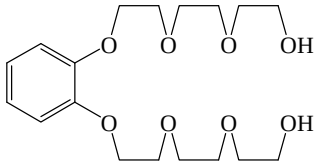

6

To a solution of **4** (5.0 g, 45 mmol) and **5** (24.5 g, 91 mmol) in acetonitrile (MeCN) (100 ml) was added K_2CO_3 (25.1 g, 182 mmol) and KI (14.6 g, 91 mmol) to form a suspension. The suspension was heated under reflux and stirred for 72 hours, leaving a brown crude suspension. The MeCN was removed *via* reduced pressure leaving a slurry. The slurry was partitioned between H_2O (100 ml) and dichloromethane (DCM) (100 ml). The DCM layer was removed and aqueous layer was extracted further using DCM (100 ml x 2). The organic layers were combined, dried ($MgSO_4$) and filtered. The filtrate was concentrated under reduced pressure. The residue was purified by column chromatography (SiO_2) using 5% MeOH in DCM. The eluent was removed under reduced pressure leaving a red oil **6** (5.28 g, 62%). ^{1}H NMR (300 MHz, $CDCl_3$); δ_H 3.49 (s, 2H), 3.75-3.61 (m, 24H) and 6.90 (m, 4H). ^{13}C NMR (100 MHz, $CDCl_3$); δ_C 60.4, 67.7, 68.2, 69.0, 69.5, 72.2, 114.2, 122.2 and147.7. MS (EI): calculated for $C_{18}H_{30}O_8$ *m/z*=374.43; found *m/z* = 397.2 $[M + Na]^+$.

Synthesis of compound 8[72].

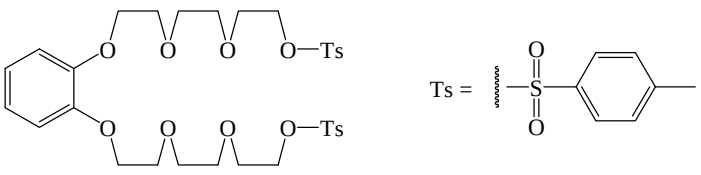

8

To a purged (N_2) reaction flask **6** (1.79 g, 4.79 mmol), triethylamine (1.93 g, 19 mmol), dry DCM (150 ml) and a sub-stoichiometric amount of 4-dimethylaminopyridine (DMAP) was added affording a solution. A solution of $_P$-toluene sulfonyl chloride (3.65 g, 19 mmol) in dry DCM (50 ml) was added drop wise at 0ºC over approximately 20 minutes. The reaction was then stirred for 6 hours and brought to ambient temperature. The DCM was removed *via* reduced pressure, re-dissolved in minimal DCM and washed with HCl (aq) (0.1 M) (100 ml x 2) and saturated NaCl (aq) (100 ml x 2). The organic layers were combined, dried ($MgSO_4$) and filtered. The filtrate was concentrated under reduced pressure. The residue was then purified by column chromatography (SiO_2) using 50/50 mix of hexane/DCM to remove first spot and 5% MeOH in DCM to remove the second spot. The eluent was removed under reduced pressure leaving a reddish oil **9** (2.75 g, 84%). ^{1}H NMR (300 MHz, $CDCl_3$); δ_H 2.39 (s, 6H), 3.55-3.59 (m, 4H), 3.63-3.67 (m, 8H), 3.78-3.81 (m, 4H), 4.09-4.14 (m, 8H), 6.88 (s, 4H), 7.3 (d, 4H, *J* = 9) and 7.75 (d, 4H, *J* = 9). ^{13}C NMR (100 MHz, $CDCl_3$); δ_C 21.6, 68.6, 68.7, 69.3, 69.7, 70.6, 70.7, 114.7, 121.6, 127.9, 229.9, 132.8, 144.9 and 148.8. MS: calculated for $C_{32}H_{42}O_{12}S_2$ *m/z*=682.21; found *m/z* (ES) = 705.5 $[M + Na]^+$, 721 $[M + K]^+$.

Synthesis of compound 10[72].

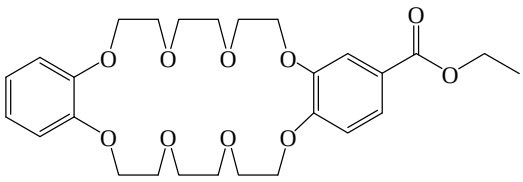

10

To a purged (N_2) reaction flask a solution of **9** (0.133 g, 0.73 mmol), K_2CO_3 (0.46 g, 3.3 mmol) and a sub-stoichiometric amount of LiBr in dry acetonitrile (MeCN) (85 ml) was heated under reflux for 1 hour. A solution **8** (0.5 g, 0.73 mmol) in dry MeCN (42 ml) was added dropwise over 30 minutes. The mixture was then heated under reflux for 72 hours and

brought to ambient temperature. Filtration and concentration of the filtrate *in vacuo* left an oil which was taken up in minimal DCM and washed with HCl (0.1 M) (100 ml x 2) and saturated NaCl (aq) (100 ml x 2). The organic layers were combined, dried ($MgSO_4$) and filtered. The filtrate was concentrated under reduced pressure, leaving a slightly brown solid. This was then recrystallised in ethanol leaving a white solid **10** (0.2 g, 52.6%). ^{1}H NMR (300 MHz, $CDCl_3$); δ_H 1.35 (t, 3H), 3.70-3.80 (m, 8H), 3.89-3.92 (m, 8H), 4.11-4.18 (m, 8H), 4.32 (q, 2H), 6.83-6.86 (m, 5H), 7.49 (d, J = 1.80Hz, 1H) and 7.63 (d, d, J_1= 1.80Hz, J_2 = 1.86Hz). ^{13}C NMR (100 MHz, $CDCl_3$); δ_C 14.4, 60.8, 69.4, 69.5, 69.6, 69.8, 69.9, 71.3, 112.0, 114.1, 114.4, 121.4, 123.8, 148.9, 166.3 and 179.8. MS (ES): calculated for $C_{27}H_{36}O_{10}$ m/z=520.23 ; found m/z = 543.2 $[M + Na]^+$, 560.2 $[M + K]^+$.

Synthesis of compound 11[73].

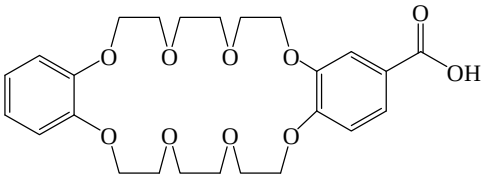

11

To a solution of **10** (0.2 g, 0.39 mmol) in ethanol (25 ml) was added potassium hydroxide (0.043 g, 0.77 mmol). The solution was then heated under reflux for 24 hours. Upon cooling to room temperature, HCl (0.1 M) was added until solution was pH = 4. Ethanol was then removed *via* reduced pressure. The resulting residue was washed with water thoroughly and dried. The resulting white solid was recrystallised from ethanol to give compound **11** (0.17 g, 90%). ^{1}H NMR (300 MHz, $CDCl_3$); δ_H 3.86-3.87 (m, 8H), 3.93-3.99 (m, 8H), 4.16-4.23 (m, 8H) 6.87-6.91 (m, 5H), 7.57 (d, J = 1.95Hz, 1H) and 7.72 (d, d, J_1= 1.98Hz, J_2 = 1.98Hz, 1H). ^{13}C NMR (100 MHz, $CDCl_3$); δ_C 69.3, 69.4, 69.6, 71.3, 71.4, 71.5, 112.0, 114.0, 114.6,

121.4, 124.8, 148.3, 148.9, 153.5 and 170.5. MS (ES): calculated for $C_{25}H_{32}O_{10}$ *m/z*=492.52; found *m/z* = 515.2 $[M + Na]^+$, 531.2 $[M + K]^+$.

Synthesis of compound 12.

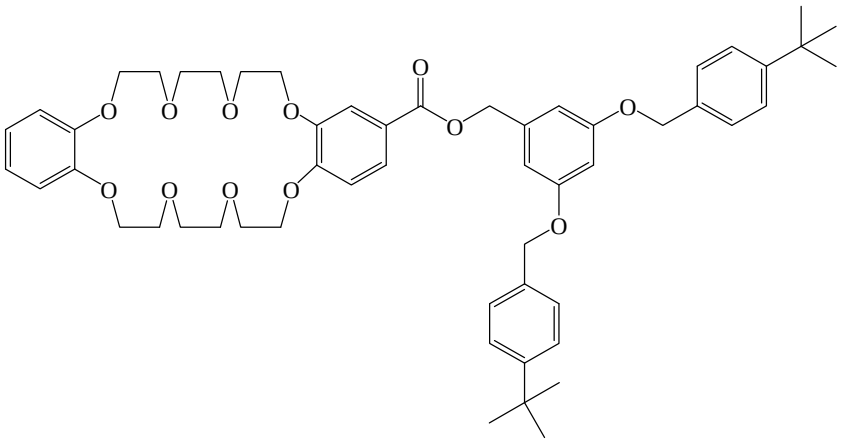

12

To **11** (0.1 g, 0.2 mmol) and **G_1** (0.088 g, 0.2 mmol), DCC (0.05 g, 0.24 mmol) and a sub-stoichiometric amount of DMAP in dry DCM (20 ml) was added at 0ºC under N_2 (gas) over 30 minutes forming a solution. The solution was then stirred under N_2 (gas) for 48 hours. The DCM was removed *via* reduced pressure. The resulting residue was purified by column chromatography (SiO_2) using DCM to remove the first spot and ethyl acetate (EA) to remove the second spot. The eluent was removed under reduced pressure leaving a white solid **12** (0.16 g, 89%). ^{1}H NMR (300 MHz, $CDCl_3$); δ_H 1.31 (s, 18H), 3.82 (m, 8H), 3.91 (m, 8H), 4.15(m, 8H), 4.98(s, 4H), 5.25 (s, 2H), 6.58 (s, 1H), 6.66 (s, 2H), 6.86 (m, 5H), 7.24-7.41 (m, 8H), 7.55 (s, 1H), 7.66 (d, 1H, *J* = 9Hz). ^{13}C NMR (100 MHz, $CDCl_3$); δ_C 31.4, 49.2, 69.4, 69.6, 71.3, 101.5, 106.9, 112.0, 114.0, 114.5, 121.4, 122.7, 124.1, 125.6, 127.6, 133.7, 138.5, 148.3, 1489, 151.1, 153.1, 160.2 and 166.1 MS (ES): calculated for $C_{54}H_{66}O_{12}$ *m/z*=906.46; found *m/z* = 929.2 $[M + Na]^+$.

7.4 Complexation Studies

Complexation 1[72]

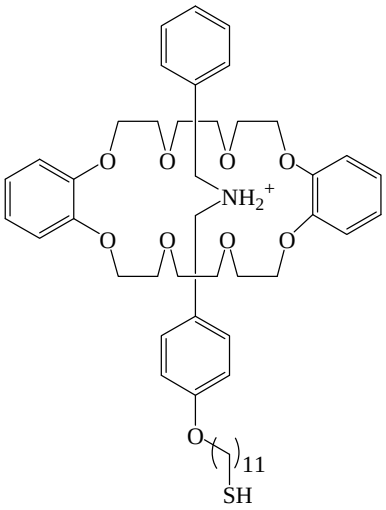

To DB24C8 (0.002 g, 4.46 µmol) in $CDCl_3$ (~2.5 ml), **1** (0.0024 g, 4.46 µmol) (synthesised by Dr Parvez Iqbal) in $CDCl_3$ (~2.5 ml) was added under N_2 (gas) forming a solution. The solution was then stirred for 24 hours. The resulting solution was then characterised by ^1H NMR. ^1H NMR indicates both complexation and starting materials present.

Complexation 2[72]

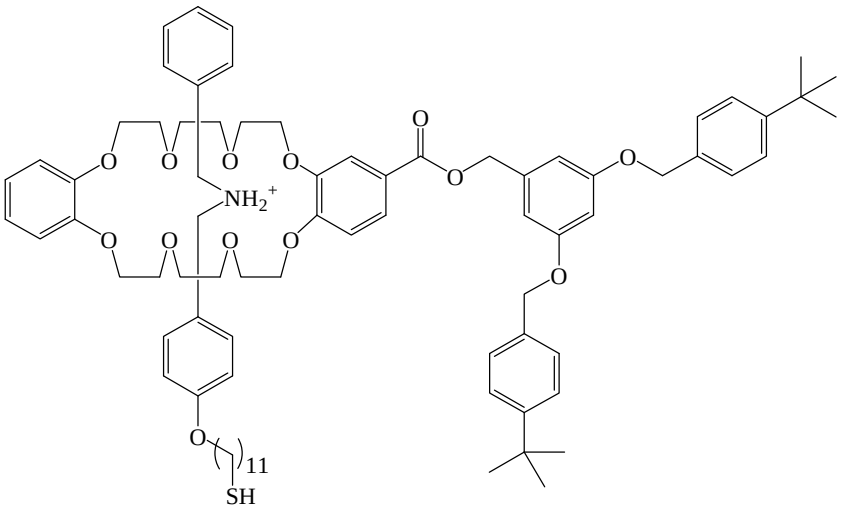

To **12** (0.14 g, 0.15 mmol) in $CDCl_3$ (~5 ml), **1** (0.082 g, 0.15 mmol) (synthesised by Dr Parvez Iqbal) in $CDCl_3$ (~5 ml) was added under N_2 (gas) forming a solution. The solution was then stirred for 24 hours. The resulting solution was then characterised by ^1H NMR. ^1H NMR indicates both complexation and starting materials present.

7.5 Surface work

7.5.1 Materials

Gold

Both the 30nm and 100nm gold were purchased from a company based in Germany called Georg Albert Physikal Vapor Disposition (PVD) (Hauptstrasse 24, Germany).

Ultra High Quality Water (UHQ H_2O)

All UHQ H_2O used for surface chemistry was supplied by a Milli-pore system at a rate of 18.2 Ω.

7.5.2 Cleaning of glassware

All organic contaminants are removed from glassware prior to use *via* a set cleaning procedure. Glassware was immersed in piranha solution (70% H_2SO_4, 30% H_2O_2) for 30 minutes[79], (*Caution*: *Piranha solution reacts violently with organic matter and should be handled with care*) rinsed and then sonicated in UHQ H_2O followed by drying in an oven at 127^{o}C for 30 minutes. Finally the glassware was rinsed, and then sonicated in ethanol for 30 minutes before being dried in the oven for 24 hours prior to use.

7.5.3 Preparation of SAMs

Au substrates were cut to a square size approximately 1 cm x 1 cm using a diamond tipped scriber. The substrates were rinsed with HPLC ethanol to clear the surface of any particles that was produced from the cutting process. The substrates were immersed into piranha solution for 10 minutes. And then rinsed vigorously with UHQ H_2O and HPLC ethanol. The rinsed substrate was immersed immediately into the desired 0.1 mM or 1 mM solution of the desired surfactants either in HPLC ethanol or HPLC chloroform for the desired time. Finally, the SAMs were rinsed thoroughly with HPLC ethanol or HPLC chloroform depending on the solvent used to make up the 0.1 mM or 1 mM solution of the surfactants and dried with a stream of $Ar_{(g)}$.

7.5.4 Characterisation of SAMs

Contact Angle

Dynamic contact angle was measured using a homemade stage apparatus, employing a charge coupled device (CCD) KP-M1E/K camera (Hitachi) which was attached to a computer for video capture. FTA Video analysis software v 1.96 (first ten angstroms) was used for the analysis of the contact angle of a droplet of UHQ H_2O at a three-phase intersection point. All contact angle measurements were recorded under ambient temperatures, humidity and pressure. All measurements were performed on 30 nm gold. Three samples were prepared for each SAM and three measurements were taken from different areas on each sample. The errors reported for the contact angle measurements are standard deviations.

Ellipsometry

Ellipsometry measurements were recorded using a Jobin, Yvon UVISEL ellipsometer with Xenon light source. A wavelength of 280-800 nm was used with a fixed angle of incidence of

70º. DeltaPsi software was used to calculate the thickness values using a cauchy oscillator model. Ellipsometer calibration and polariser alignment was conducted using a Al reference sample which had a thermally grown Al_2O_3 layer. All measurements were done on 100 nm gold.

XPS

XPS spectra were obtained on the Scienta ESCA300 instrument based at the Council for the Central Laboratory of the Research Councils (CCLRC) in The National Centre for Electron Spectroscopy and Surface Analysis (NCESS) facility at Daresbury, UK. XPS experiments were carried out using a monochromatic Al K_α X-ray source (1486.7 eV) and a take off angle of 15°. Fitting of XPS peaks was performed using the *Avantage* V*2.2* processing software.

7.5.5 SAM Formation

SAM Formation of TEGT

Clean gold substrate was immersed in a 0.1 mM solution of TEGT in HPLC ethanol for either 2 hours, 4 hours, 8 hours, 16 hours and 24 hours. All samples were characterised by dynamic contact angle and ellipsometry with the 24 hour sample also being characterised by XPS.

SAM formation of dialkyammoniumthiol

Clean gold substrate was immersed in a 1 mM solution of dialkylammonium thiol in HPLC chloroform for either 2 hours, 4 hours, 8 hours, 16 hours and 24 hours. All samples were characterised by dynamic contact angle and ellipsometry with the 24 hour sample also being characterised by XPS.

7.5.6 Control Studies

Control study 1

Clean gold substrate was immersed in a 1 mM solution of **12** in HPLC ethanol. At the same time clean gold substrate was immersed in HPLC ethanol. All samples were immersed for 24 hours and characterised by ellipsometry.

Control Study 2

Clean gold substrate was immersed in a 1mM solution of dialkylammonium thiol, **1** (**figure 3.1**) in HPLC chloroform for a period of 24 hours. A sample was then characterised by ellipsometry and contact angle. Another sample was rinsed vigorously with HPLC chloroform and immersed in a 0.1 mM solution of TEGT, **2** (**figure 3.1**) for a further 24 hours. The sample was then characterised by contact angle and ellipsometry.

8.0 References

1. P. Macnaghten, M. B. Kearnes, B. Wynne, *Science Communication*, **2005**, 27, 268.
2. P. Iqbal, PhD Thesis, *University of Birmingham*, **2006**, Ch1.
3. R. P. Feynman, *http://www.zyvex.com/nanotech/feynman.html*., **1960**.
4. N. Taniguchi, *Proc. Intl. Conf. Prod. Eng. Tokyo*, **1974**, *II*.
5. P. Ball, *Nature*, **2000**, 406, 118.
6. A.L. Nielsen, K. Steffensen, K. L. Larsen, *Colloids and Surfaces B: Biointerfaces*, **2009**, 73 267-275.
7. A. Ulman, *An introduction to organic thin films from Langmuir – Blodgett to Self-Assembly*, **1991**, Academic Press INC
8. P. M. Mendes, J. A. Preece, *Current Opinion in Colloid and Interface Science*, **2004**, *9*, 236-248.
9. J. C. Love, L. A. Estroff, J. K. Kriebel, R. G. Nuzzo, G. M. Whitesides, *Chem. Rev.*, **2005**, 105, 1103-1170.
10. O. Bolduc, J. F. Masson. *Langmuir*, **2008**, 24, 1285-12091.
11. S. Diegoli, C. A. E. Hamlett, S. J. Leigh, P. M. Mendes, J. A. Preece, *Aerospace Engineering*, **2007**, 221, 589-620.
12. P. Mendes, *Chem. Soc. Rev.*, **2008**, 37, 1-18.
13. F. Schreiber, *J. Phys.: Condens. Mater.*, 2004, **16**, R881.
14. A. N. Parikh, B. Liedberg, S. V. Atre, M. Ho, D. L. Allara, *J. Phys. Chem.*, **1995**, 99, 9996.
15. C. K. Luscombe, H. W. Li, T. S. Huck, A. B. Holmes, *Langmuir*, **2003**, 19, 5273.
16. N. Tillman, A. Ulman, J. S. Schildkraut, T. L. Renner., *J. Am. Chem. Soc.*, **1988**, 110, 6136.

17. J. Lahann, S. Mitragotri, T. N. Tran, H. Kaido, J. Sundaram, I. S. Choi, S. Hoffer, G. A. Somorjai, R. Langer., *Science*, **2003**, 299, 371.

18. P. E. Laibiris, G. M. Whiteside, *J. Am. Chem. Soc*., **1992**, 114, 9022.

19. M. Mrksich, *Chem. Soc. Rev.*, **2000**, 29, 267.

20. U. Makal, K. J. Wynne, *Langmuir*, **2005**, 21, 3742-3745.

21. C. K. Luscombe, H. W. Li, W. T. S Huck, A. B. Holmes, *Langmuir*, **2003**, 19, 5273-5278.

22. P. M. Mendes, M. Belloni, M. Ashworth, C. Hardy, K. Niktin, D. Fitzmaurice, K. Critchley, S. Evans, J. A. Preece, *Chem. Phys. Chem.*, **2003**, *4*, 884.

23. H. Basch, M. A. Ratner, *J. Chem. Phys.*, **2004**, *120*, 5771-5780.

24. F. Schreiber, *Progress in Surface Science*, **2000**, 65, 151-256

25. D. Hobara, M. Ota, S. I. Imabayashi, K. Niki, T. Kakiuchi, *Journal of Electroanalytical Chemistry*, **1998**, 444, 113-119.

26. E. W. Wollman, C. D. Frisbie, M. S. Wrighton, *Langmuir*, **1993**, 9, 1517.

27. C. D. Frisbie, L. F. Rozsnyai, A. Noy, M. S. Wrighton, C. M. Lieber, *Science*, **1994**, 265, 2071.

28. E. W. Wollman, D. Kang, C. D. Frisbie, I. M. Lorkovic, M. S. Wrighton, *J. Am. Chem. Soc.*, **1994**, 116, 4395.

29. X. M. Yang, D. A. Tryk, K. Ajito, K. Hashimoto, A. Fujishima, *Langmuir*, **1996**, 116, 5525.

30. G. P. Lopez, H. A. Biebuyck, G. M. Whitesides, *Langmuir*, **1996**, 10, 1498.

31. M. J. Tarlov, D. R. F. Burgess, G. Gillen, *J. Am. Chem. Soc.*, **1993**, 115, 5305.

32. A. Kumar, H. A. Biebuyck, G. M. Whitesides, *Langmuir*, **1994**, 10, 1498.

33. G. Gillen, S. Wright, J. Bennett, M. J. Tarlov, *Appl. Phys. Lett.*, **1994**, 65, 534.

34. H. A. Biebuyck, G. M. Whitesides, *Langmuir*, **1994**, 10, 4581.

35. C. D. Bain, G. M. Whitesides, *J. Am. Chem. Soc*., **1988**, 110, 3665.

36. C. D. Bain, G. M. Whitesides, *J. Am. Chem. Soc*., **1989**, 111, 7164.

37. H. A. Biebuyck, G. M.Whitesides, *Langmuir*, **1993**, 9, 1766.

38. C. D. Bain, G. M. Whitesides, *Angew. Chem. Intl. Ed*, **1989**, 28, 506.

39. V. V. Demidov, *Expert Review of Molecular Diagnostics*, **2004**, 4, 267-268.

40. K. L. Prime, G. M. Whitesides, *Science*. **1991**, 252, 1164.

41. P. Harder, M Grunze, R. Dahint, G. M. Whitesides, P.E. Laibinis, *J. Phys. Chem.* **1998**, 102, 426.

42. J. Piehler, A. Brecht, R. Valiokas, B. Liedberg, G. Gauglitz, *Biosensors & Bioelectrics*, **2000**, 15, 473-481.

43. J. M. Harris, *Introduction to biotechnical and biomedical applications of poly(ethylene) glycol*, **1992**, New Youk: Plenum Press. 1-14

44. K. V. Gujraty, R. Ashton, S. R. Bethi, S. Kate, C. J. Faulkner, G. K. Jennings, R. S. Kane, *Langmuir*, **2006**, 22, 10157-10162.

45. S. Choi, W. L. Murphy, *Langmuir*, **2008**, 24, 6873-6880.

46. R. K. Smith, S. M. Reed, P. A. Lewis, J. D. Monnell, R. S. Clegg, K. F. Kelly, L. A. Bumm, J. E. Hutchison, P. S. Weiss, *J. Phys. Chem.B.*, **2001**, 105, 1119-1122.

47. S. J. Stranick, A. N. Parikh, Y. T. Tao, D. L. Allara, P. S. Weiss., *J. Phys. Chem*., **1994**, 98, 7636-7646.

48. D. Hobra, M. Ota, S. I. Imabayashi, K. Niki, T. Kakiuchi, *Journal of Electroanalytical Chemistry*, **1998**, 444, 113-119.

49. J. K. Whitsell, H. K. Chang, *Science*, **1993**, 261, 73.

50. F. Diederich, L. Echegoyen, M. G. Lopez, R. Kessinger, J. F Stoddart, *J. Chem. Soc., Perkin Trans.2,* **1999**, 1577-1586.

51. D. A. Tomalia, K. Mardel, S. A. Henderson, G. Holan, R. Esfand, *Dendrimers – An enabling synthetic science to controlled organic nanostructures in Handbook of Nanoscience, Engineering and Technology*, **2003**, CRC Press.

52. B. J. Hong, J. Y. Shim, S. J. Oh, J. W. Park, *Langmuir*, **2003**, 19, 2357-2365.

53. H. Tokuhisa, J. Liu, K. Omori, M. Kanesato, K. Hiratani, L. A. Baker., *Langmuir*, **2009**, 25, 1633-1637.

54. J. M. Lehn, *Angew. Chem. Int. Edit. Engl.*, **1990**, 29, 1304-1319.

55. P. R. Ashton, P. T. Glink, J. F. Stoddart, P. A. Tasker, A. J. P. White, D. J. Williams, *Chem. Eur. J.*, **1996**, 2, 729-736.

56. C. J. Pedersen, *Angew. Chem. Int. Ed. Engl.*, **1988**, 27, 1021-1027.

57. P. R. Ashton, R. A. Bartsch, S. J. Cantrill, R. E. Hanes, S. K. Hickingbottom, J. N Lowe, J. A. Preece, J. F. Stoddart, V. S. Talanov, Z. H. Wang, *Tetrahedron lett.*, **1999**, 40, 3661-3664.

58. R. E. Gillard, F. M. Raymo, J. F. Stoddart, *Chem. Eur. J.*, **1997**, 3, 1933-1940.

59. C. J. Pedersen, *J. Am. Chem. Soc.*, **1967**, 89, 7017-7036.

60. P. R. Ashton, P. J. Campbell, E. J. T. Chrystal, P. T. Glink, S. Menzer, D. Philp, N. Spencer, J. F. Stoddart, P. A. Tasker, D. J. Williams, *Angew. Chem. Int. Ed. Engl.*, **1995**, 34, 1865-1869.

61. D. Philp, J. F. Stoddart, *Angew. Chem. Intl. Ed. Engl.*, **1997**, 97, 1154-1196.

62. P.R. Ashton, M. C. T. Fyfe, S. K. Hickingbottom, J. F. Stoddart, A. J. P.White, D. J. Williams, *J. Chem. Soc. Perkin. Trans 2.*, **1998**, 2117-2128.

63. S. Angelos, Y. W. Yang, K. Patel, J. F. Stoddart, J. I. Zink., *Angew. Chem. Int. Ed.*, **2008**, 47, 1-6.

64. N. K. Mal, M. Fujiwara, Y. Tanaka, *Nature*, **2003**, 421, 350-353.

65. K. C. F. Leung, T. D. Nguyen, J. F. Stoddart, J. I. Zink, *Chem. Mater.*, **2006**, 18, 5919–5928.

66. R. Hernandez, H. R. Tseung, J. W. Wong, J. F. Stoddart, J. I. Zink, *J. Am. Chem. Soc.*, **2004**, 126, 3370-3371.

67. S. Saha, K. C. F. Leung, T. D. Nguyen, J. F. Stoddart, J. I. Zink, *Adv. Funct. Mater.*, **2007**, 17, 685-693.

68. B. H. Northrop, A. B. Braunschweig, P. M. Mendes, R. W. Dichtel, J. F. Stoddart, *Molecular Machines. In Handbook of Nanoscience, Engineering and Technology*, CRC Press, **2007**.

69. A. W. Adamson, *Physical Chemistry of Surfaces 5th Edition*, Wiley Interscience (Chichester), **1990**.

70. L. I. Maissel, R. Glang, (Editors), *Handbook of Thin Film Technology*, *McGraw-Hill (New York)*, **1970**.

71. J. F. Moulder, W. F. Stickle, P. E. Sobol, K. D. Bomden, *Handbook of X-ray Photoelectron Spectroscopy*, **1992**.

72. F. Diederich, L. Echegoyen, M. G. Lopez, R. Kessinger, J. F. Stoddart, *J. Chem. Soc. Perkin Trans.2*, **1999**, 1577-1586.

73. D. J. Feng, X. Q. Li, X. Z. Wang, X. K. Jiang, Z. T. Li., *Tetrahedron*, **2006**, 60, 6137-6144.

74. I. C. Goncalves, M. Cristina, L. Martins, M. A. Barbosa, E. Naeemi, B. D. Ratner, *J. Biomed. Mater. Res.*, **2008**, 642-653.

75. C. Palegrosdemange, E. S. Simon, K. L. Prime, G. M. Whitesides, *J. Am. Chem. Soc.*, **1991**, 113, 12-20.

76. B. Zhu, T. Eurell, R. Gunawan, D. Leckband, *J. Biomed. Mater. Res.*, **2001**, 56, 406-416.

77. S. Shuquing, P. Mendes, K. Critchley, S. Diegoli, M. Hanwell, S. D. Evans, G. J. Leggett, J. Preece, T. H. Richardson, *Nano. Lett.*, **2006**, 6, 345-350.

78. A. Ulman, *Chem Rev.*, **1996**, 96, 1533-1554.

79. C. S Lee, S. E. Baker, S. M. Marcus, S. W. Yang, M. A. Eriksson, R. J. Hamers, *Nano Lett.*, **2004**, 4,1713-1716.